PHYSICAL PROPERTIES OF CENOSPHERE

A Thesis submitted in partial fulfilment of the requirements

for the award of the Degree of

Master of Technology

in

Geotechnical Engineering

Civil Engineering Department

by

SUBHARJIT SEN

212CE1063

DEPARTMENT OF CIVIL ENGINEERING

NATIONAL INSTITUTE OF TECHNOLOGY

ROURKELA - 769008

MAY 2014

PHYSICAL PROPERTIES OF CENOSPHERE

A Thesis submitted in partial fulfilment of the requirements

for the award of the Degree of

Master of Technology

in

Geotechnical Engineering

Civil Engineering Department

by

SUBHARJIT SEN

212CE1063

Under the guidance of

Prof. Chittaranjan Patra

DEPARTMENT OF CIVIL ENGINEERING

NATIONAL INSTITUTE OF TECHNOLOGY

ROURKELA - 769008

MAY 2014

Department of Civil Engineering
National Institute of Technology
Rourkela – 769008
Odisha, India
www.nitrkl.ac.in

CERTIFICATE

This is to certify that the thesis entitled "**Physical Properties of Cenosphere**" submitted by **Mr. Subharjit Sen** (Roll No. 212CE1063) in partial fulfilment of the requirements for the award of Master of Technology Degree in Civil Engineering with specialization in Geo-Technical Engineering at National Institute of Technology, Rourkela is an authentic work carried out by him under my supervision and guidance.

To the best of my knowledge, the matter embodied in the thesis has not been submitted to any other University / Institute for the award of any Degree or Diploma.

Date:

Place:

Dr. C R Patra
Professor
Department of Civil Engineering
National Institute of Technology
Rourkela – 769008

Acknowledgment

I am heartily thankful to my supervisor, Dr. C.R.Patra, whose encouragement, supervision and support from the preliminary to the concluding level enabled me to develop an understanding of the subject.

I cannot fully express my gratitude to the exceptional team at Department of Civil engineering, NIT Rourkela including my friends. I am really thankful to Dr. Dillip KumarPradhan, for his generosity, faith and superb guidance. I extend my thanks to Ph.D. scholars Mr. Satya Narayan Tripathy, Mr. Tapabrata Dam, Mr. Ashutosh Pattanaik and Mr. Sumanta Kumar Sahoo for their co-operation. For the generous assistance in the research of this project, I would like to acknowledge the Department of Metallurgical and Material Science for providing the required lab set up for my sample preparation, Department of Physics for required slot for dielectric measurement and XRD and Department of Ceramics engineering for FESEM.

Lastly, I express my deepest gratitude to my parents, brother and my friends for their moral support and love.

Subhrajit Sen

Roll No-212ce1063

Department of Civil engineering

NIT, Rourkela

Rourkela-769008

Content Pages

III.Chapter-3: Experimental Technique

IV.Chapter-4: Results and discussion

Abstract

Cenospheres are exclusive free flowing powders comprised of hard shelled, hollow, tiny spheres collected from coal ash. Their amount is based on the C and Fe content present in the fly ash. Due to lower value of thermal conductivity, higher particle strength, ultra-low density, impermeability they are used in various industries. However, it is necessary to study the various physical properties of these ash particles for its improved and effective usage. In the present study, systematic investigation of the structural, microstructural, thermal, electrical and mechanical properties of cenosphere have been carried out. X-ray diffraction studies reveal the primary constituents of cenosphere. Quartz, mullite, sillimanite, magnetite, hematite, rutile, dipotassium oxide, calcium oxide, sodium oxide, magnesium oxide are the primary constituent of cenosphere. FESEM micrographs indicate that cenosphere is a hard shelled hollow space. Plerosphere is also found in the light weight particle. Complex impedance spectroscopy has been employed to analyze the bulk properties of the material. The room temperature dielectric study shows the high electrical resistivity property. The frequency dependent dielectric spectroscopy confirms polar characteristics of cenosphere. The average diameter of cenosphere is around 100μm. TGA and DTA thermogram of cenosphere reveals the higher thermal stability of cenosphere. Cenosphere is stable up to 1000°C with negligible mass loss. The endothermic peak around 300°C reveals decomposition of carbonaceous material in cenosphere. Compressive strength of cenosphere has been carried out. Compressive strength of cenosphere pellet produced by 6 ton loading is around 7.38 MPa.

LIST OF FIGURES

LIST OF TABLES

Chapter-1

Introduction

INTRODUCTION

1.1 What is Cenosphere?

Coal fired boilers are extensively used to produce steam for production of electricity. A common form of boiler uses a pulverized coal that is injected into a furnace. Fly ash is produced by of burning coal in boiler. Some of the improved fly ash is commercially utilizable in concrete, concrete products, cement production, sewage sludge stabilization, pavement base materials, lightweight aggregate, reinforced plastics, and other miscellaneous purposes. The residual fly ash must usually be disposed of by land filling since it has hardly any commercial value. It is well acknowledged that landfill space is quickly failing in many regions and that the construction of new landfills is very expensive. In this way, much endeavor has been administered at discovering utilization for fly ash remains with the goal that the fly ash does not require to be land filled and any usable item from this waste material is praiseworthy. Depending on the composition of coal the composition of fly ash varies. Therefore, to be used in specific applications material specifications have been developed for this waste material. The particular shows that these waste particles are made for the most part of silicon dioxide, aluminum oxide and iron oxide. Different types of structures are observed in the particles in fly ash. A few particles in fly ash are strong. Different particles in fly ash are empty and are called cenospheres.

The expression "cenosphere" is determined from two Greek words, kenos (empty) and sphaira (sphere). Cenospheres are lightweight, idle, and empty circles basically comprising of silica and alumina, are loaded with air or gasses, and are by results of the ignition of pulverised coal at the warm power plants.

A cenosphere is a lightweight, idle, empty sphere made to a great extent of silica and alumina and loaded with air or inactive gas, commonly processed as a by-result of coal burning at warm power plants. Cenospheres fluctuates from light black color to practically white shade and their specific gravity extends in the middle of 0.4–0.8 g/cm^3, which offers them extraordinary lightness.

Another variety of the particles, present in the coal ash, are called ‘plerosphere’. Plerosphere derived from two words pleres (filled) and sphaira (sphere). The cavity is filled with ash particle and/or other materials in plerosphere. Both cenosphere and plerosphere are combined termed as ‘microsphere’. These microspheres alongside the powder enter fiery debris settling reservoirs, where because of their low thickness; they are amassed generally at the outside surface, and might be easily headed out by sprinkle and wind. Microspheres have

various interesting properties that give prospects to their successful use in numerous propelled innovations. This upgrades the need to enhance the routines for their assembly, the deeper examination of the properties and systems of their arrangement, and working out the ideal states of usage.

1.2 Uses of cenosphere

Cenospheres are basically thin-walled hollow spherical particles with relative density of less than 1.0. They are floated on water and are recovered from the float up of ash disposal lagoons and are similar chemical composition as that of fly ash. Cenosphere are used in various industries due to their unique combination of spherical shape, high compression, low specific gravity, good thermal and acoustical insulation properties and inertness to acids and alkalis.

These are some of the examples of uses of cenosphere in different industries around the globe.

These are 75% lighter than different minerals at present utilized as fillers like clay, talc & calcium carbonate and so forth and are 30% lighter than generally pitches. The high finished result of cenosphere is unmanageable tiles of space boats, flying machine coatings and oil well bonds.

Ceramics: Refractories Tile, fire Bricks, insulating materials, coatings, Aluminum cement.

Plastics: Injection moldings, film, nylon, HDP, LDP, PP, PVC flooring etc.

Construction: Specialty cements, roofing materials, acoustical panels, coatings, mortars etc.

Recreation: Marine craft, flotation devices, golf equipment, footwear, garden décor, mortars etc.

Automotive: Composites, under water coatings, body fillers, sound proofing materials, engine parts, brake pads, tires etc.

Energy & Technology: Cements used in oil well cement for its impermeable property, industrial coating, aerospace coating, and propeller blades etc.

These are some of the examples of composites of cenosphere.

Ashref: These cenosphere based refractories are light and have splendid thermal shock properties. In spite of their relatively low cool pounding quality, they can bear 30 cycles, in which they are then again warmed to 1100°c and cooled to 25°c, without exasperating their structural integrity.

Alulite: This is a saturated matrix complex of cenosphere and calcined alumina. Alulitehas the hardness of high alumina tiles, but is relatively light in nature and has better thermal

shock resistive property. With the raise in cenosphere content in the compound strength of the composite is increased.

Keralite: This cenosphere-based hard-headed comprises of an arrangement of empty spheres and is melded at their purpose of contact. It is a gigantically troublesome item to produce because of the little shear resistance of the cenospheres. Creative aptitude has been urbanized to make Keralite. Because of the substantial cenosphere stacking they are more expensive than their rivals.

Hollocast: A customary unmanageable castable with cenospheres, which streams amazingly well under vibration and can even consume fine detail in a mould. It has demonstrated enough effective as furnace furniture, and likewise demonstrates certification as a hot face lining for ferrosilicon spoons for diminishing sculling. Vermiculite-based "semi-protection" assets of the same warm conductivity have a density of 1.35 g/cm^2 however accomplish less quality.

Constituents of cenosphere

- SiO_2 (Quartz):

Molar mass of SiO_2 is 60.08 g/mol. Density of this transparent crystal is 2.648 g/cm^3. It has high boiling point in between 1600°-1725°C. As it is the prime constituent of cenosphere the hollow spherical particle contains higher thermal resistivity. In fused silica state it has compressive strength of 1100MPa. Quartz is used in the production of Portland cement, drinking glasses, glass for windows and beverage bottles. It finds its application in telecommunication industry in the manufacture of optical fibre. For removal of tooth plaque it can be used in hydrated form in toothpaste.

- Al_2O_3 (Alumina):

It is found in crystalline form having molecular mass of 101.96 g/mol. Its density and melting points are 4.1 g/cm^3 and 2072°C respectively. It has high compressive strength value of 1900-2000 N/mm^2. It is an inert compound. For this inertness it is used as filler in plastic industry and for its high electrical resistivity it is used as electrical insulator.

- Fe_2O_3 (Hematite):

Hematite is a rhombohedral crystal structure material with higher density of 5.24 g/cm^3 and having molecular mass of 159.69 g/mol. It is the main raw material for steel and iron industries. It is used in final polishing of lenses and jewellery.

- CaO (Calcium oxide):

Calcium oxide is a widely used compound commonly known as quicklime. It is an alkaline crystal solid. It is white in color. It is soluble in water. It has molecular mass of 56.0774 g/mol and possess of higher melting point of 2613°C. Quicklime finds its application in numerous industries like light, cement, paper, chemical production etc. It is used in light industry for its ability to produce intense glow when the material is heated to 2400°C.

- TiO_2 (Rutile):

Titanium oxide is found in mineralogical form in nature and is commonly known as rutile. The molar mass of the compound is 79.866 g/mol. It possesses density of around 4.23 g/cm^3. Its important application areas are in paper, plastic, paints and varnish industries. Rutile is also used in production of glass, electrical conductor, and cosmetic industry. It is widely used in sunscreen for its ability to block UV rays due to its high refractive index.

- MgO (Periclase):

The mineralogical form of magnesium oxide is known as periclase. It has molar mass of 4.3044g/mol, density around of 3.85g/cm^3 and higher melting point. Periclase mineral is used in fire refractory, medicine, desiccant and cement industries.

- P_2O_5 (Phosphoric acid):

Phosphoric acid is a white colored powered having density 2.39 g/cm^3. P_2O_5 sublimates at 360°C. It is soluble in water. It is used as a dehydrating agent. For oxidation of alcohol Phosphoric acid is mixed with dimethyl sulphoxide. It contains some injurious properties. This material is highly inflammable in nature and has metal corrosive properties.

1.4 Thermal Analysis

Thermal Analysis is the term applied to a group of methods and techniques in which chemical or physical properties of a material, a mixture of substances or a reaction combination are considered as a function of temperature or time, in which the substances are subjected to a controlled temperature programme.

1.4.1 Uses of Thermal Analysis Techniques:

- to measure a property of interest, such as specific heat, latent heat or heat of reaction
- to fingerprint a particular material or substance
- to measure the high-temperature stability of materials
- to notice phase transformations

- for fundamental studies of reaction kinetics

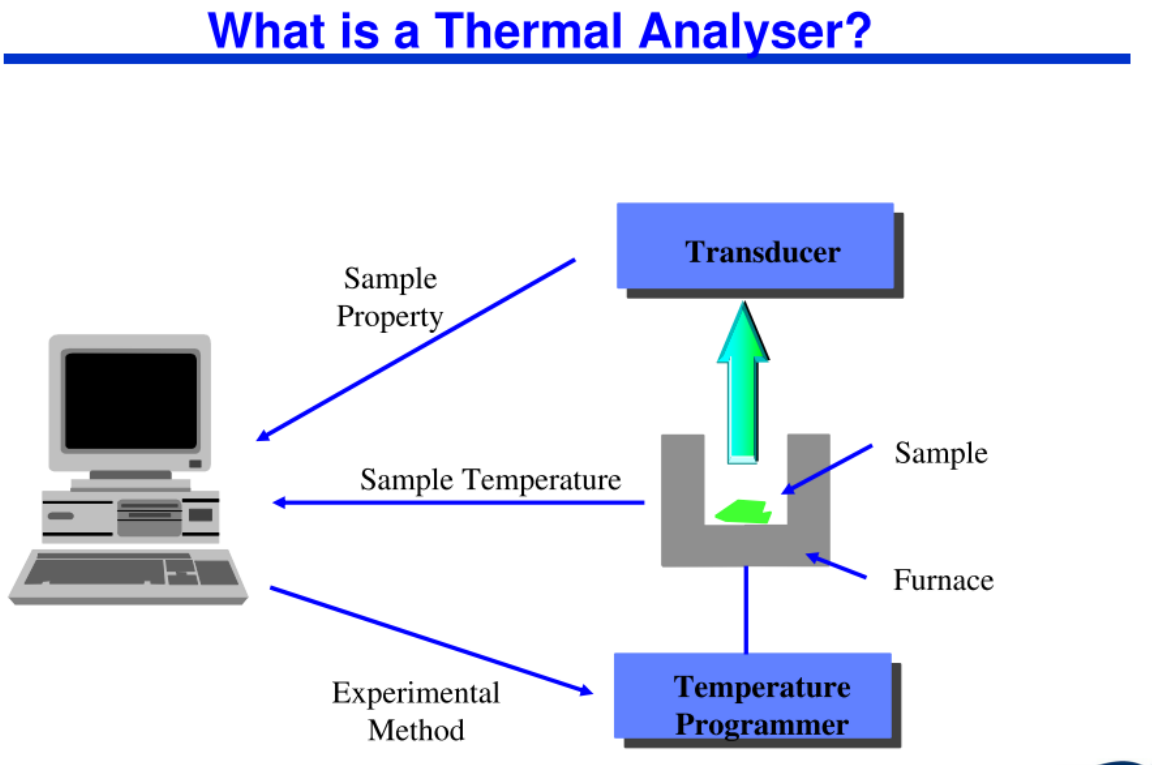

1.1 Thermal Analyser

1.4.2 Thermal Analysis Instruments:

All the thermal analysis instruments have features in common. The example held in a suitable specimen dish or crucible, is set in a heating furnace and subjected to some sought of temperature program.

Throughout this methodology, one or more properties of the specimen are observed by utilization of suitable transducers for changing over the properties to electrical parameters, for example, voltage or current.

The assortment of the methods to be examined stems from the mixture of physical properties that might be measured and the variety of transducers of transducers that could be utilized.

Estimations are normally consistent and the heating rate is regularly, but not so much, linear with time.

The results of such measurements are thermal analysis curve sand the feature of this curves (peaks, discontinuities, change of slopes etc.) are related to the thermal events in the samples.

1.4.3 Thermogravimetry:

Thermogravimetric analysis is a technique in which the change in mass of the materials under examination is continuously recorded as a function of temperature as it is heated or cooled at the programmed rate.

The temperature programme is most often a linear increase in temperature, but, also be carried out, when the changes in sample mass with time are followed.

TGA is innately quantitative, and hence to a great degree capable heating method, yet gives no direct chemical data. The ability to analyze the volatile products during a weight loss is of great value

1.4.4 Presentation of TGA data:

In a mixture of graphical courses, results from TG analyses might be introduced. Mass or mass percent is for the most part plotted as the ordinate (Y-axis) and temperature or time as the abscissa (X-axis). Mass percent has the advantage that the results from different experiments can be compared on normalized sets of axes. At the point when time is utilized as the abscissa, a second bend of temperature versus time needs to be plotted to show the temperature system utilized. Derivative plot used to find points of inflection. Thermogravimetric curves or TG curves permits evaluation of thermal stabilities, rate of reaction, reaction processes, and composition of the sample.

1.4.5 Instrumentation of Thermal analyzer:

Thermogravimetric instrumentation should include several basic components to provide the flexibility necessary for the production of useful analytical data:

- A balance, (Thermo balance/microbalance)
- heating device, (Furnace)
- A unit for temperature measurement (Sensor) and control, (Temperature programmer)
- Temperature sensor: Thermocouple placed close to the sample
- Temperature programmer: A typical operating range for the furnace is ambient to 1500°C, with heating rates up to 200°C/min.

1.4.6 The Thermobalance:

Measurements of changes in sample mass with temperature are made using thermobalance.

The balance should be in a suitably enclosed system so that the atmosphere can be controlled.

Several types of balance mechanism are possible:

- Measurement of deflection.
- Null point weighing mechanism.

- Balances must remain precise and accurate continuously under extreme temperature and atmosphere conditions, and should deliver a signal suitable for continuous recording.
- ✓ Null-deflection weighing mechanisms are favoured in TG as they confirm that the sample remains in the same zone of the furnace regardless of changes in mass.
- ✓ Sensitivity of balance ≈1g for a 1g maximum load balance.
- ✓ The output weight signal may be differentiated electronically to give a derivative thermogravimetric curve (DTG).

1.4.7 Differential Thermal Analysis (DTA):

This is a widely used technique which is simple to perform and understand.

- ✓ Differential: It refers to the difference between two physical quantities (e.g. the temperatures of sample and reference material for DTA) under a controlled temperature program.
- ✓ Differential thermal analysis is a technique which accounts the dissimilarity in temperature (ΔT) between a substance and a reference material against either time (t) or temperature whilst the two specimens (i.e., the substance and reference material) are subjected to identical temperature in an environment heated or cooled at a controlled rate.
- ✓ Samples are generally in the 1–10mg range for analytical applications.
- ✓ DTA measures temperature difference between a sample and an inert reference while heat flow to the reference and the sample remains the same.
- ✓ The sample of interest (S) and an inert reference (R) are placed in the same furnace and hence are subject to the equal heat treatment.
- ✓ There is a single block with symmetrical cavities for sample and reference is heated in the furnace.

- ✓ The square is decided to go about as a suitable high temperature sink, and an example holder of low thermal conductivity is incorporated between the sample and the specimen to guarantee a satisfactory differential temperature indicator throughout a heating events.
- ✓ Less than 10 mg of sample (s) and inert reference (r) are contained in Al pans each with thermocouple, held in heating block, with thermocouple. The type of thermocouple used for the differential measurement is critical since the measured temperature differences can be quite small.
- ✓ The temperature difference between the sample and reference is measured by a differential thermocouple, in which one junction is contact with the underside of the sample crucible and other is underside of the reference crucible.
- ✓ The DTA experimental set up consists of two thermocouples connected in series: one junction is immersed in the sample cell while the other is immersed in reference (generally alumina) cell. The reference and sample are contained in a same metal block, which is heated at a linear-heating rate.
- ✓ The sample temperature is measured via the voltage across the appropriate screw terminals (VT1) and similarly for reference temperature (VT2). Then the temperature difference between the sample and reference is measured by a differential thermocouple with difference in temperature (VΔT).
- ✓ Sample and reference temperature measurements require cold junction temperature corrections. The most critical component of a good DTA is the differential thermocouple signal amplifier, which must amplify minute voltages while eliminating random noise.
- ✓ The output of the differential thermocouple, Ts-Tr or ΔT, is amplified and sent to the data acquisition system. This permits the difference in temperature between the sample and the reference to be recorded as a function of the sample temperature, the reference temperature or time.
- ✓ If there is no contrast in temperature, no indication is produced, despite the fact that the genuine temperatures of the specimen and reference are both expanding.
- ✓ Operating temperatures for DTA instruments are by and large room temperature to something like 1600 ˚c; some DTA mechanical assembly are fit for working from -150˚ C to 2400˚c. To achieve the precise low sub-surrounding temperatures, a liquid nitrogen cooling embellishment is required. Some low temperatures (but, not -1500˚c) may be arrived at with electrical cooling gadgets or with constrained air-cooling.
- ✓ Heating the furnace at a programmed rate raises the temperature of the sample and the reference. Energy is absorbed or liberated, altering the heat flux through the heat-sensitive

plate and inducing a temperature difference between the sample and the reference, when the sample undergoes a phase transformation. In the event that the example experiences a physical change or a chemical response, its temperature will change despite the same temperature of the reference material remains. That is on account of physical changes in a material, for example, phase changes and chemical reactions typically include changes in enthalpy, the high temperature substance of the material.

1.4.8 Data Presentation:

DTA curve plots the temperature difference as a function of the programmed furnace temperature in the scanning mode or as a function of time in the isothermal mode.

- ✓ In DTA curve, ΔT is usually plotted on the ordinate and T or t on the abscissa increasing from left to right.
- ✓ Since the definitions of ΔT as Ts-Tr is rather arbitrary, each DTA curve should be marked with either the endo or exo directions.
- ✓ For the DTA curve, the temperature difference (ΔT) should be plotted on the ordinate with endothermic reactions downwards.
- ✓ There is a constant temperature difference ΔT between s and r since they have different heat capacities. But when the sample undergoes any reactions then change ΔT becomes different.
- ✓ Schematic illustration of the measured sample temperature as a function of time for a polymer subjected to a linear heating ramp, and the corresponding DTA curve.
- ✓ If a sample doesn't undergoes a thermal reaction over the temperature range involved, a continuous recording of the temperature difference (ΔT) between the sample and the reference should result in a baseline parallel to the temperature axis (i.e., ΔT = constant value).
- ✓ However if a sample experiences an endothermic reaction (i.e., the temperature of the sample falls below that of the reference materials so that ΔT is negative) such as phase transition or melting temperature, the plot of ΔT vs. T(t) will produce a deflection from the base line and subsequent return to the base line in the form of an endothermic peak.
- ✓ Conversely, if a sample undergoes an exothermic reaction, the heat evolved will cause an increase in the temperature of the sample compared to that of the reference resulting an exothermic peak (ΔT is positive).

1.4.9 Reference Materials:

The reference material should have the following characteristics:

- The reference material should undergo no thermal events over the operating temperature range.
- The reference material should not react with the sample holder and thermocouple.
- Both the thermal conductivity and the heat capacities of the reference should be alike to those of the sample.
- Alumina (Al2O3), Carborundum, SiC have been widely used as references substances for inorganic samples, while for organic compounds, especially polymers, use has been made of Octyl phthalate silicon oil.

Both solid examples and reference material are generally utilized as a part of powder structure. The particle size and packing conditions influences results. There should not any reaction between sample and reference materials.

1.5 Electrical resistivity

1.5.1 Origin of resistance:

The electrical resistance of an object is an amount of its opposition to the passage of an electric current. Electrical resistance of a circuit element or device is well-defined as the ratio of the voltage applied to the electric current which flows through it.

$$R = \frac{V}{I}$$

Ohm (Ω) is the SI unit of electrical resistance. Electrical conductance is the reciprocal quantity of resistance which is measured in Siemens.

1.5.2 Resistivity:

The quantitative measure of a material's opposition to the flow of current is called resistivity. It depends only on the composition of the material and not on the shape and size.

$$R = \frac{\rho L}{A}$$

Where,

R is the resistance (ohms),

ρ is resistivity (ohm-meters),

L is length (meters), and

A is cross-sectional area (square-meters).

1.5.3 Resistivity measurement methods:

The resistivity is calculated by measuring resistance R and the measurements of the sample (length l, width w and thickness d). The resistance R is determined by a voltage-current method. A current of known 'I' value is fed into the sample and the voltage 'V' is measured via point connection.

From these measurements the resistivity is determined as,

$$\rho = R\frac{w * d}{l}$$

Here two probe method is used for resolve of resistance.

1.5.4Two probe method:

The test specimen for the two probe method may be in the form of strip, rod or bar. The two probe method usually gives a value with contributions from contact wires, contact resistance and hence not sensible in case of metals where the sample resistance is very low.

Since the internal resistance of voltmeter is very high (10^6 Ω), hence $I_o << I$, so the voltage measured by the voltmeter will be,

$$V = (I - I_o)(r + R + r)$$

So, r+R+r give an error to the measurement. However this method can be applied (if R>>2r) for high resistive samples.

1.5.5Dielectric constant:

The dielectric constant is the ratio between permittivity of a substance and permittivity of free space. It is an estimation of the degree to which a material concentrates electric flux. It is the electrical equivalent of relative magnetic permeability.

As the dielectric constant increases, the electric flux thickness expands, gave all different components stay unaltered. This permits objects of a given size, such as sets of metal plates is used hold their electric charge for long periods of time, and/or to grip large amounts of charge. High-value capacitors are made from materials with high dielectric constants.

1.5.6: Loss tangent:

The dielectric loss tangent is characterized by the angle between the capacitor's impedance vector and the negative reactive axis. It concludes the lossiness of the medium.

Like dielectric constant, low loss tangent is resulted as “fast” substrate while large loss tangents result in a “slow” substrate.

$$\varepsilon = \varepsilon_{R_o} + j\varepsilon_{Im}$$

The dielectric constant can be evaluated using: $\varepsilon = C_s / C_v$, where C_s is the capacitance with the specimen as the dielectric, and C_v is the capacitance with a vacuum as the dielectric. The dissipation factor can be evaluated using: $D = \tan\delta = \cot\theta = 1 / (2\pi f R_p C_p)$, where θ is the phase angle, δ is the loss angle, f is the frequency, and C_p is the equivalent parallel capacitance and R_p is the equivalent parallel resistance.

Chapter-2

Literature study and objective

LITERATURE STUDY AND OBJECTIVE

Recently several experimental investigations have been devoted to structural, microstructural, thermal and mechanical properties of cenosphere by different research groups around the globe.

2.1 **Literature study:**

Ghosal Sarbajit and Sidney A. (1994) conducted studies on particle size-density relation and cenosphere content of coal fly ash of various site. Cenosphere was collected from six different sites and centrifugal separation method was used to classify the ashes into six different density categories ranges from 1.6 to 3.2 g/cm^3. The size distributions of all densities classed were determined in the range 1 to 200μm. With increasing particle density, the cenosphere size increases. Centrifugal separation using a liquid of density 2.2 g/cm^3 was used to estimate the mass fraction of cenosphere. The cenosphere fraction varied from 5 to 95%. The median diameters of the microspheric fractions were found to be two to three times those of non-microspheric fractions.

Kolay and Singh (2000) studied the physico, chemico and mineralogical behavior of the cenospheres obtained from an ash lagoon. Cenosphere particle consists of smaller percentages in the pulverized coal ash. They concluded that cenosphere particles are light weight particles and their specific gravity is very low. Cenosphere is thermally stable upto 280°. The cenosphere particles are noticed to be almost uniform in size and their specific surface area is quite low.

Stanislav V. Vassilev *et al.* (2003) studied the morphological characterization of cenosphere. They conducted experiments by taking cenosphere from five sites and found that highest percentage of cenosphere obtained between 20 and 300μm. They found that the recovered ceramic cenospheres are in the range of 0.2-1.1% of the total fly ash. Their phase-mineral mainly consists of aluminosilicate, calcite, rutile, mullite, quartz, cristobalite, hematite, char and plagioclase.

Zhi-qiu Huang *et al.* (2010) suggested the behavior of AZ91D Mg alloy/fly-ash cenospheres composites. They fabricated AZ91D Mg alloy/fly-ash cenospheres by metal stir technique. 100μm size cenosphere particles were used with mass fraction of 4%, 6%, 8% and 10%. The effects of mass fraction of cenospheres on the microstructure and compressive properties were characterized. They found that cenospheres are uniformly distributed in the matrix. The densities of composites were in the range of 1.858-1.92g/cm^3.They found that the hardness of AZ91D/FAC composites increases with increasing the content of the

cenospheres. They concluded that the compressive strength of composite is higher than that of as cast AZ91D Mg alloy. The composites containing 4% of cenosphere gives the higher compressive strength and higher yield strength is observed in composites containing 8% of cenosphere.

Wang Mei-Rong *et al.* (2011) conducted experiments on microstructural and mechanical characterization of cenosphere fabricated with metakaolin based geopolymer. They studied thermal, mechanical and microstructural properties of cenosphere. Cenosphere did not dissolve in highly alkaline solution. It was observed that bulk density, thermal conductivity and mechanical strength properties of the composites decreased monotonically with increase of FAC in the composites. It was concluded that lower thermal conductivity and lesser density can be achieved in the metal composites with a slight decrease in the mechanical strength by the addition of FAC.

Dou Z. Y. *et al.* (2007) revealed the high strain compression behaviour of cenosphere when fabricated with aluminium syntactic foams. The syntactic foam exhibits distinct train rate of sensitivity and increase in peak strength. From this experiment cenosphere shows the greater energy absorbing properties. The composites show 45-60% of higher dynamic compressive strength than that of quasi-static compression.

Ngu L. *et al.* (2007) characterized the fly ash cenosphere obtained from various Australian Power Stations. This research revealed that iron is not the essential constituent of the fly ash from which cenosphere is formed. Cenosphere particle has larger diameter and nearly 70% of cenosphere falls in the range between 45 and 150μm. Both single-ring and network like structure were observed in the spherical sample. Single-ring like structure was the majority percentages than that of network like structures. The smaller spherical sized particle contains higher value of SiO_2/Al_2O_3 ratio than that of larger sized cenosphere. The wall thickness to diameter of the light weight particle lies in between an upper bound of 10.5% and lower bound of 2.5%. It is revealed that large ash cenosphere has lower SiO_2/Al_2O_3 value. Larger range of spherical particle mainly forms network like structure.

Xian M. and Shen X. (2012) found that metal alloys can be coated on cenosphere by heterogeneous precipitation method. Magnetic binary alloy coated cenosphere can be produced by thermal reduction of the composites in N_2/H_2 atmosphere at temperature range of 700° C. The uniformly binary coating is obtained on the cenosphere surface and the binary allocated spherical composites retained the spherical morphology. It is suggested that binary alloy coating can be made up to multilayer by successful fabrication. The composites exhibit

higher value of coercivity than that of pure binary alloy. The composites exhibit higher values of magnetic shielding and higher microwave absorption properties.

Alcala J.F.C. *et al.* conducted research on methods and condition of cenospheres obtain form fly ash in thermal power plant. Around 1.7% cenosphere was obtained from fly ash. The batch settling procedure was employed to get the cenosphere from fly ash. The cenosphere obtained in the process shows large spherical portion. It was found that they have hollowness and sometimes the bigger cenosphere was filled with lesser diameter cenosphere particle.

Gurupira T. *et al.* extracted the cenosphere from fly ash by the triboelectric separation method. Larger sized particles were separated from fly ash by mechanical sieving in which triboelectric separator was used. Lithium metatungstate solution was used along with distilled water centrifugation for recovery of the spherical hollow particles.

Majkrzak G. *et al.* (2007) performed experiment on compressive strength of cenosphere. It was concluded that cenosphere brick was much lower density and much more durable to alternate freeze/thaw environment. It was observed that by replacing cenosphere 10% by weight with the fly ash lowered the density from 2.07 to 1.71g/cc. Lower weight bricks are used for architectural design and reduction of handling and labour cost. The freeze/thaw durability confirms the improve insulating thermal properties.

Shukla A. *et al.* (2001) studied the compressive strength, flexural strength and tensile strength of cenosphere blended with asphalt and cement. It was concluded with the addition of cenosphere loses the strength of concrete and ultimately lowered the density. This strength loss was recovered by improving the interfacial strength between the cenosphere and the cement producing high strength lightweight concrete. The loss in strength of cenosphere-cement composite can be regained with suitable interface modifier such as silica fumes. Cenosphere was coated with Styrene-Acrylonitrile and Styrene-Butadiene polymer and their strength properties were studied.

Tiwari V. *et al.* (2004) studied the acoustical properties of cenosphere blended with asphaltic and reinforced cement concrete. The experimental study revealed that noise reduction efficiency can be improved by addition cenosphere up to 40%. Sound absorption property of asphaltic concrete decreases with increase in cenosphere content, and normal acoustic impedance increases with an increase in cenosphere volume fraction.

2.1 Main Objectives

The proposed work is based on the following objectives.

1. Preparation of the sample after the recovery from ash lagoon.
2. Studies of structural and microstructural properties of cenosphere.
3. Studies of particle size distribution and morphological analysis of cenosphere.
4. Study of compressive strength property of hollow sphere.
5. Studies of thermal stability behaviour and surface area analysis of cenosphere.
6. Study of complex impedance spectroscopy of cenosphere at room temperature.
7. Study of dielectric responses as a function of frequency at room temperature.
8. Study of compositional analysis of fly ash cenosphere.

Chapter-3

Experimental Procedure

EXPERIMENTAL TECHNIQUE

The basic principles and various experimental techniques used in this work are discussed briefly in this chapter. As the sample is directly collected from ash lagoon this requires suitable cleaning procedure for the future study. The experimental techniques include mineralogical analysis, surface morphology, resistivity study, compositional study, thermal analysis, particle size distribution study.

3.1 Sample Preparation

As cenosphere was directly recovered from the ash lagoon they contain so much of impurities. So it should be cleaned to carry out further experimentation.

To remove the contaminants on the surfaces of cenosphere particles and improve the dispersion of the particles, the cenosphere particles were first cleaned with CH_2Cl_2 solution at room temperature for 10 min.200ml.of $CH_2Cl_2$was taken in a beaker and 50gm.of cenosphere particles were added to it. The cenosphere particles obtained from the above cleaning process were taken into further cleaning by treating with weak alkali followed by rinsing three times with deionized water.0.3 mol/L NaOH solution was prepared by taking 1000ml of water along with 12gm. of NaOH. The cenosphere was added to weak alkali (0.3 mol/L NaOH) followed by ultrasonication for 30 minutes. After 30 minutes the treated cenospheres were taken and rinsed with deionized water for three times. The cenosphere obtained by treating with weak alkali were further treated with weak acid followed by rinsing with deionized water. 1% HCl solution was prepared by adding 10ml of HCL with 990ml of water. The cenosphere was added to that weak acid solution followed by stirring for 15 minutes. After 15 minutes the cenosphere was taken from the acid solution and rinsed with deionized water for three times. The above treated cenosphere was then oven dried at 105^0celsius for 10 hours.

3.1.1 Why these chemicals are used in the cleaning process?

- Dichloromethane (CH_2Cl_2):

Dichloromethane is an organic compound having molecular formula CH_2Cl_2. It is used in the cleaning process as declusterizing agent. The cenosphere collected from ash lagoon was found in clustered state due to accumulation of moisture. So for proper cleaning it should be first made to single-ring like structure. As dichloromethane is used as a degreaser it can eradicate the impurities in the sample. The density of dichloromethane is 1.33g/cm^3. So the impurities in the light weight particle can be easily settled down in the organic solvent.

- Sodium hydroxide (NaOH):

Sodium hydroxide known as caustic is frequently used as a cleaning agent in various industries. It lowers the surface tension on the surface of the cenosphere particle and thus removes the impurities which were left after the organic solvent treatment. Caustic can dissolve fat, oil and grease from the treated sample.

- Hydrochloric acid (HCl):

Hydrochloric acid is used to neutralize the sample after treated with dil. Sodium hydroxide. As HCL has melting point and boiling point below normal room temperature so HCL got vaporize leaving behind the clean cenosphere. The dil. Hydrochloric acid is used to clean any metal particle left in the sample.

3.1.2 Why ultrasonication is used in the sample synthesis?

It is the process in which sound energy of frequency of more than 20 kHz is applied to agitate the sample. Ultrasonication is used for loosening the particles which are adhering to the cenosphere surface. The dil. Sodium hydroxide lowered the surface tension of adhering particle and ultrasonication is used to remove the unwanted surfactant by loosening the bond between them.

3.2 Particle size distribution

The most important physical property of particulate samples is particle size. Particle size measurement is regularly carried out across a wide range of industries and is often a critical parameter in the production of many products. Particle size is helpful in different industries for its application towards reactivity or dissolution rate, flow ability and handling capacity, viscosity, and stability in suspension, appearance, efficacy of delivery, texture, packing density and porosity properties.

The particle size of the fly ashes was measured using a laser based particle size analyzer, named as Mastersizer 2000 of Malvern Instruments Ltd. Fraunhofer diffraction of light formed by particles with a diameter larger than the incident laser beam wavelength is utilized in this instrument. It combines an optical filter, lens and photo detector which hare coupled with a computer loaded with Mastersizer software enables one to compute the particle size distribution from the diffraction data and store it as volume percentage against the particle size.

Figure 3.1: Dynamic Light Scattering Zeta Sizer: Malvern Instrument

Definition: A suspension of powder in isopropanol is measured with a low angle laser beam, and it calculates the particle size distribution.

Scope: This is a fast method for measuring particle size distribution of powders.

Principle: The method can be used on all powders containing less than 10% fat.

Apparatus

- Malvern Instrument
- Malvern QS Small Volume Sample Dispersion Unit.
- Malvern in/out measuring cell, beam length 2.0 mm.
- Dispenser 0-50 ml with container.
- Filling knife.
- Waste container.

Reagents

- Isopropanol, IPA (technical quality).

Procedure

✓ The instrument is Prepared for measuring in wet mode using IPA as the liquid, as described in the user manual. The stirrer regulator should be set at 2000 rpm on the Malvern unit.

- ✓ Quickly a sufficient amount of milk powder is added and measurement is taken as soon as the powder is dispersed and not later than 20 seconds after addition of the powder.
- ✓ All measurements are completed in duplicate.

Result

The subsequent calculations are made automatically:

- The volume median diameter D (v, 0.5) is the diameter where 50% of the distribution is above and 50% is below.
- Two determinations of mean particle size should not differ by more than 5% relative. The shape of the curves in the two determinations should be the same.
- D (v, 0.9), 90% of the volume distribution is below this value.
- D (v, 0.1), 10% of the volume distribution is below this value.

3.3 Specific surface area

Specific surface area is the total surface area of a material per unit of mass of solid or bulk volume or cross-sectional area. It is a derived scientific value which is used to determine properties of a material (e.g. soil). It is well-defined either by surface area divided by mass (with units of m^2/kg), or surface area divided by the volume (units of m^2/m^3 or m^{-1}). Here Blaine air permeability apparatus has been used for the evaluation of surface area of the sample.

Apparatus:

Blaine air permeability apparatus comprised of a manometer, a stainless steel permeability cell, a perforated metal disk, and a stainless steel plunger.

Balance – 0.001g resolution

Timer – 0.5s resolution.

Materials:

Cenosphere- 1.5 g

Filter paper

Manometer Liquid – light grade of mineral oil (low viscosity and density).

Procedure:

1) Approximately 4gm. of cenosphere is placed in a small covered jar or tin container. It is shaken vigorously for 2 minutes to fluff the cenosphere and break up lumps and agglomerates. The covered container is allowed to stand for 2 minutes, then remove is covered and gently stirring is done to homogenize the sample.

2) The perforated metal disk is gently seated in the permeability cell on the ledge at the bottom of the cell using a rod having a diameter slightly smaller than that of the cell. A filter paper is placed on the metal disk and is pressed down with this same rod.

3) The cenosphere is placed in the cell on top of the first filter paper. The side of the cell lightly tapped in order to level the bed of cenosphere. A second filter paper is placed on this bed of cenosphere.

4) The cenosphere is compressed with the plunger until the plunger collar contacts the top of the cell. Slowly the plunger is withdrawn to a short distance; the plunger is rotated to 90°, and the cenosphere is compressed a second time until the collar is contacted the top of the cell. The plunger is slowly removed. It is noted that fresh filter papers must be used for each determination.

5) The permeability cell is attached to the manometer tube (a little is used stopcock grease to ensure an airtight connection).

6) The air in the right arm of the manometer is slowly evacuated using the pressure bulb until the liquid is reached the top mark, and then the manometer valve is closed. The liquid will start to slowly lower because of airflow through the cement sample into the manometer.

7) The timer is started when the bottom of the meniscus of the liquid reached the second mark from the top and the timer is stopped when the bottom of the meniscus reached the third mark (next to the bottom mark). This time, T, is recorded to the nearest 1 second.

Calculation:

The specific surface area (S) of the sample has been obtained with the help of Eq.3.1

$$S = \frac{S_s \text{ x } (n_s)^{1/2} \text{ x } (T)^{1/2}}{(T_s)^{1/2} \text{ x } (n)^{1/2}}$$

Equation-3.1

S_s=Specific surface area of the standard sample used in the calibration of the apparatus

n_s=Viscosity of air in poises at temperature of test of the standard sample used in the calibration of the apparatus

n= Viscosity of air in poises at temperature of test of the test sample

T= Measured time interval, in seconds, of manometer drop for test sample

T_s=Measured time interval, in seconds, of manometer drop for test sample used in the calibration of the apparatus.

Here Portland cement has been taken as the reference material for standardization.

Figure 3.2: Blain's air permeability apparatus

3.4 Compressive strength

Approximately 3 gm. weight of sample is taken and few drops of water were added to it to give some extra binding property. Water content varied between 10–20 drops.

Then the die was cleaned with cotton followed by acetone so that all the dust is removed from the inside surface of the die and outside surface of the punch. Then greasing was done to avoid sticking. Then the cenosphere powder prepared earlier was poured inside carefully. During the packing slight shaking was done to accommodate the maximum possible amount of material. Then the whole system was subjected to hydraulic press. Then load of 4 tons is applied on it very slowly. Then the load was kept constant for 5 min at 4 ton. Three samples were prepared by the above process.Similarly another three samples were prepared by the same process described above, by the load application of 6 tons.

These are some of the images of the instrumental set up.

Figure 3.3: Uniaxial Compessive strength testing machine

Figure 3.4: Dye

Figure 3.5: Pellets

3.5 Compositional analysis

- **SiO_2:**

0.5g of sample is taken and filled with 4-5g of KOH pellets (Nickel crucible). It is then extracted with hot H_2O (50ml). 25ml of conc. HCl and 10ml of HNO_3 are added and boiled until appearance of a transparent solution. Solution is cooled and transferred to a plastic beaker. 1g of NaF and KCl is added till the solution gets saturated. It is then filtered through filter paper 42 and washed with washing solution till the filter paper become acid free. The filter paper along with the residue is then transferred to the plastic beaker. Washing solution is added to it and then kept in ice bath for 10minutes. Bromothymol blue indicator is added to it till the solution changes to orange colored and then it is titrated with NaOH N/15 till blue colour appears. 250ml neutral boil water is taken and titrated against NaOH N/15

taking Bromothymol blue as indicator. The neutral boiled H_2O along the washing solution containing filter paper is boiled in water bath for 30 minutes. Bromothymol blue indicator is added to it and then titrated against NaOH N/15 till blue colour appears. This consumption of NaOH is noted. In the same way blank is prepared.

Calculation:

Actual NaOH consumption= consumption in the sample - consumption in the blank

$$SiO_2\% = \frac{1.505 * V * N}{\text{wt.of the sample}}$$

V= Vol. of NaOH consumed

N= Strength of NaOH

- **Al_2O_3:**

25ml. of stock solution is pippeted. 25ml EDTA solution is added to it. 2-3 drops of methyl orange indicator is added. 1:1 NH_3 solution is added till the solution gets colourless. Dilute HCl (1:1) is added drop wise to change the colour to pink. Again 1:1 NH_3 solution is added till the solution gets colourless. 10ml of buffer solution is added. The solution is boiled and then cooled. Then again 10ml. of buffer solution is added to it. Xylene orange indicator is added and titrated against 0.02M zinc acetate till the colour is changed to red. 1 spoon of NaF is added and boiled and cooled. 2ml. of CH_3COOH is added. Again Xylene orange indicator is added and titrated against 0.02M zinc acetate till the colour is changed to red.

Calculation:

Burette reading (BR) * Factor * 2

(Of 0.25g sample is taken)

- **Fe_2O_3:**

From stock solution 10ml solution is taken in a conical flask. 10ml of conc. HCl is added to the solution. The solution is boiled for 5 minutes to reduce the solution. 5% $SnCl_2$ is added drop wise in hot condition till the solution become colourless. The solution is cooled immediately after addition of excess one drop of $SnCl_2$. Excess $SnCl_2$ is removed by addition of 10ml saturated $HgCl_2$. The solution is appeared as a silky white solution. 20ml of mineral alloy is added. 3-4 drops of BDS (barium diphenylamine sulfonate) is added and titrated against $K_2Cr_2O_7$ (0.5N) till appearance of deep violet colour.

Calculation:

$$Fe_2O_3\% = \frac{BR * N * 79.85(\text{factor})}{10 * \text{sample weight}(10 * \frac{1}{250})}$$

3.6 X-ray diffraction (XRD)

X-ray diffraction is a process to determine the mineralogical and micro structural constituent of material. X-ray diffraction is a non-destructive method which based on Bragg's law of diffraction. In this analytic technique crystal is indented a beam of X-ray and subsequent diffraction angles and intensities are evaluated. The orientations of electron densities are measured in the crystal from the diffracted data. The average spacing between the planes is measured in this method. The shape and size of the material is estimated by this analytical technique. Goniometer is the instrument used for X-ray diffraction

Bragg's law of diffraction:

Bragg's law regulates the angle between incident rays and diffracted rays. Bragg's law is expressed as:-

$n * \lambda = 2d\sin\theta$

n= an integer

λ=wavelength of incident rays

d=spacing between the planes

θ=angle between incident rays and diffracted rays

Constructive interference of diffracted beams occurs, when Bragg's law is satisfied. 'Bragg's reflection' is picked up by detector at this scanning angle at the constructive interference. The interlayer spacing in the crystal structure of the atoms is determined by the 'Bragg's reflection'. The contribution towards the reflection regulates the peak intensities in this analytical method.

Three things can be determined from an XRD pattern are:

(1) The relative positions of the diffraction peaks determine the size and shape of the unit cells.

(2) Atomic positions within the unit cell are determined by the relative intensities of the diffraction peaks electron (charge density distribution).

(3) Peak broadening is associated with microstructural parameters.

Application of X-ray diffraction:

Identification: X-ray diffraction technique is used for identification of unknown sample. Identification for materials can be done in various temperature phases, solid solution and resolve the unit cell parameter of new material.

Polymer crystallinity:

A polymer exists in both crystalline phase and amorphous phase. The crystalline phase is dominated by reinforced grid like structures. The crystalline part gives sharp narrow peak and the amorphous part is determined by broad peak.

Texture analysis:

Texture analysis is the determination of the preferred course of crystallites in polycrystalline solid. The preferred orientation is usually described in terms of pole figures. For the constant reflection at different angular orientation of the sample different diffraction intensities are taken with the function of angular orientation of particle the contour map of intensity is plotted. The h, k, l plane in the crystal is determined from this contour map. This h, k, l values give the plane texture of sample.

Measurement of lattice parameter, grain size and thermal expansions are determined by X-ray diffraction. This analytic technique can measure the relative thickness of thin films and multi layers.

For understanding the various properties of the materials the accurate determination of lattice parameters provides an important basis. The calculation of lattice constants from the line positions (2θ) or d spacing can be estimated from a generalized formula:

$$\frac{1}{d_{hkl}^2} = V^2(h^2b^2c^2\sin^2\alpha + k^2c^2a^2\sin^2\beta + l^2a^2b^2\sin^2\gamma)$$

$$V = \text{ unit cell volume} = abc(1 - \cos^2\alpha - \cos^2\beta - \cos^2\gamma + 2\cos\alpha\cos\beta\cos\gamma)^{1/2}$$

Where *a, b, c, α, β* and *γ* are lattice parameters and *h, k, l* are the Miller indices. Using the above formula, lattice parameters for all the compositions were found out.

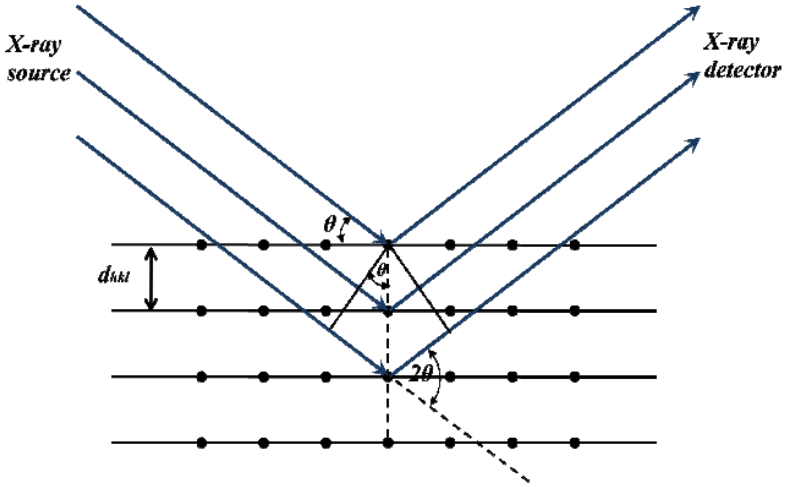

(Figure 3.6: Bragg's reflection from crystallographic planes)

3.7 Field emission scanning electron microscope

The field emission scanning electron microscopy is a non-destructive imaging technique to study the morphology of the material with very high resolution. When a beam of highly energetic electron strikes any material, the secondary electrons, x-rays and back scattered electron are ejected from the sample. Those expelled electrons are collected by a detector and convert them into signal that displays on screen. FESEM is modified version of SEM with 3 to 6 times higher resolution than the previous one. This provides a narrower probing beam. It offers both low as well as high electron energy concentration. It reveals spatial variations in chemical compositions provide qualitative chemical analyses and identifies crystalline structures. Advantages of a Scanning Electron Microscope are its wide-array of applications, the complete three-dimensional and topographical imaging. It can give the approximate size of particle in specific ranges. The morphological analysis technique causes improved spatial resolution and minimize sample charging and damage. In the present study NOVA NANOSEM 450 and SEM, JOEL, JSM840A (Japan) have been used with gold plated sample.

3.8 Energy dispersive X-ray spectroscopy

Energy dispersive x-ray spectroscopy is an analytic technique used for the characterization of chemical constituent of the sample. It uses the x-ray spectrum emitted by specimen sample bombarded with a beam of electrons for chemical characterization. All elements ranging from atomic number 4 to 92 can be detected by EDS method. Qualitatively analysis involves the identification of the spectral lines. Quantitative analysis entails measuring line intensities meant for each element in the sample and for the same elements in calibration standards of known composition. In the present study SEM, JOEL, JSM840A (Japan) have been used with gold plated sample.

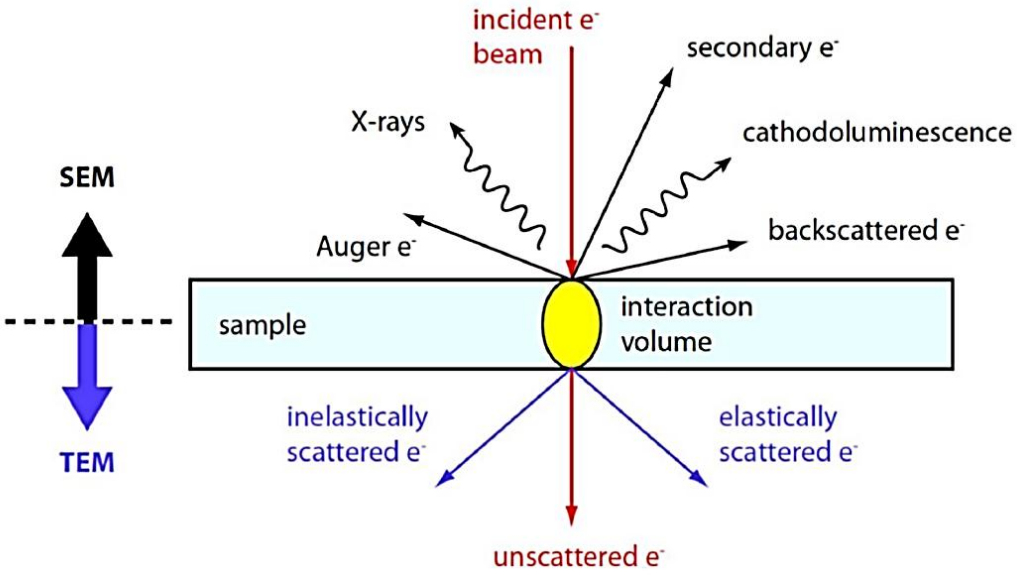

(Figure 3.7: Interaction of electron beam with specimen)

3.9 Thermal Analysis

Thermal analysis is a study of experimental condensed matter physics where the properties of the materials are investigated as a function of temperature. There are a large number of thermal analysis methods providing information regarding various aspects of the materials such as: phase transitions, transition temperature, heat of reaction, oxidative stability, purity, thermal stability, creep/stress relaxation, flexural modulus, energy dissipation, permittivity and loss factor etc. In practice thermal analysis gives properties like; enthalpy, thermal capacity, mass changes and the coefficient of heat expansion. Solid state chemistry uses thermal analysis for studying the reactions in the solid state, thermal degradation reactions, phase transitions and phase diagrams. Among various thermal analysis techniques, thermogravimetry analysis (TGA) and differential thermal analysis are included in our study for analysis purpose.

TGA is basically used to determine the amount and the rate of weight change in the material as a function of temperature in a controlled atmosphere. The measured weight loss curve gives information on: (a) changes in sample composition (b) thermal stability (c) kinetic parameters for chemical reactions in the sample. Thermal events do not bring about a change in the mass of the sample, such as melting crystallization and glass transition cannot be detected by TGA, but those accompanying mass change, such as decomposition, sublimation, reduction, desorption, absorption and vaporization can be determined by this technique.

DTA as the name implies, is a technique involving the measurement of heat effect in a specimen while subjecting to a temperature scan. The heat effects are detected by measuring the differences in heat flow into or from the sample and a reference material as a function of temperature. Since the reference is thermally inert in the temperature range of interest, such measurement facilitates isolation of heat effect in the samples from the heat taken up for rising temperature of the specimen and its surroundings. The rate of heat exchange between the sample and its surroundings (while it undergoes a transition) can, therefore, be suitably amplified and recorded. DTA is employed to determine the quantity of heat that is either absorbed (endothermic) or released (exothermic) by a substance undergoing a physical or chemical change.

The simultaneous application of TG and DTA to the same sample in a single instrument provides more information due to the perfectly identical test conditions. In the present study, we have used NETZSCH analyzer for thermal analysis. Sample was heated in a platinum pan from room temperature to 1000 °C at a heating rate of 10 °C/min under N_2 atmosphere.

3.10 Dielectric Property Measurement

When electric field is applied to a dielectric material it becomes polarized due to induced dipole moment or reorientation of permanent dipole moments (local re-arrangement of charge) present in the sample. Under an external electric field (E), the electric displacement vector (D).

$$D = \varepsilon E = \varepsilon_0 E + P$$

Where ε is the dielectric permittivity and P is called the polarization (dipole moment per unit volume) and can be expressed as.

$$P = \chi_e \varepsilon_0 E$$

Where χ_e is the electric susceptibility and ε_0 is the free space permittivity (8.85×10^{-12} F/m).The induced dipole moment (P) is directly proportional to applied field (E) (low field magnitude) and by combining the above two equations, it can be written that

$$\frac{\varepsilon}{\varepsilon_0} = \varepsilon_r$$

Where ε_r is named the relative permittivity.

The dielectric permittivity or relative permittivity is a complex quantity in an alternating electric field and it is written as:

$$\varepsilon_r^* = \epsilon^{/} + \epsilon^{//}$$

where the real part $\epsilon^{/}$ is known as dielectric permittivity or dielectric constant and the imaginary part $\epsilon^{//}$ is related to the energy loss in the system.

When a dielectric is laid open to the ac voltage, the electrical energy is absorbed by the material and is dissipated in the form of heat. The dissipation is termed as dielectric loss. In this case, the current leads the voltage by (90-δ), where δ is called the loss angle and tanδ is the electrical loss better known as tangent loss (See Figure 3.8).

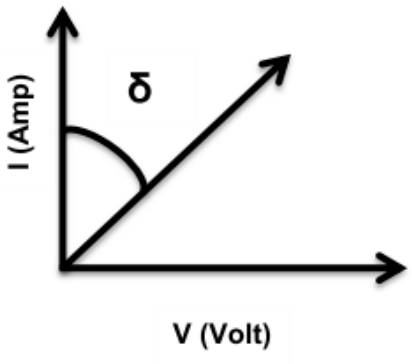

Figure3.8: Phase diagram between current and voltage

Loss tangent can be expressed as:

$$tan\delta = \frac{\epsilon^{//}}{\epsilon^{/}}$$

The dielectric property of a system highly depends on the frequency and temperature because of the various polarization mechanisms and as a consequence, resonance and relaxation effects occur as a function of frequency. Resonance is occurred at the time of the applied frequency is in the same range as the relaxation time.

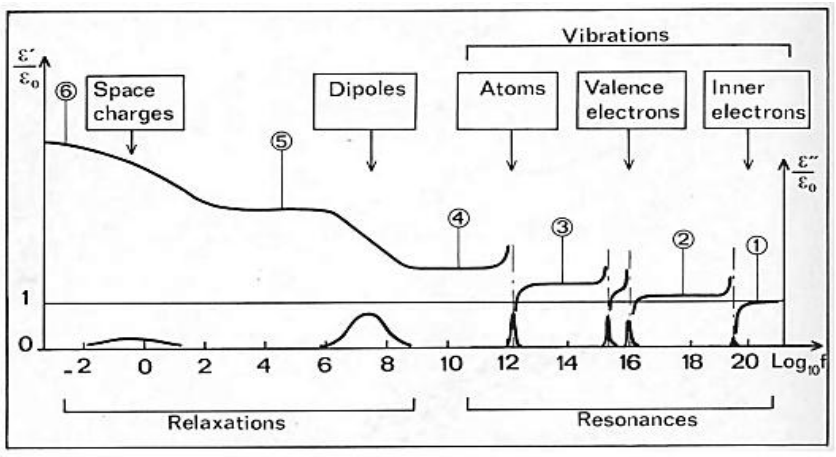

Figure 3.9: Variations of $\boldsymbol{\epsilon}^{/}$ and $\boldsymbol{\epsilon}^{//}$ with frequency

3.11 Complex Impedance Spectroscopy

Complex impedance spectroscopy (CIS) is an experimental technique used to examine, analyze and interpret electrical response of a polycrystalline sample in a wide range of frequencies. The technique analyses the ac response of a system to a small perturbation, and following estimation of the impedance as a function of the frequency. This technique also enables us to evaluate and separate the contribution to the overall electrical properties in frequency domain due to electrode reactions at the electrode/material interface, the migration of charge carriers (ions) through the grains and across the grain boundaries within the sample. The display of impedance data in the complex plane plot appears in the form of a succession of semicircles attributed to relaxation phenomena with different time constants due to the contribution of grain (bulk), grain boundary and interfacial polarization in a polycrystalline material. Hence, the contributions to the overall electrical property by various electrical phenomena in the material are separated out easily.

AC electrical data may be represented in any of the four basic formalisms which are interconnected to each other

$$\text{Complex impedance: } Z^* = Z' - j\,Z''$$

$$\text{Complex admittance: } Y^* = (Z^*)^{-1}$$

Where $j=\sqrt{-1}$, $\omega=2\pi f$ is the angular frequency and $C_0 = \varepsilon_0\, Ad^{-1}$ in which C_0 is the vacuum capacitance of the cell without the sample. *A* and *d* are the sample effective area and thickness respectively.

There are several ways of presenting the data and the most common are as follows. (a) plots of the real and imaginary components either in logarithmic or in linear coordinates against frequency, (b) polar plots of the imaginary component against the real component on a linear presentation. The type of relaxation can be understood by shape of the plot as Debye, Cole–Cole, Cole–Davidson *etc.*, and also as a means of finding the equivalent circuit for the material. The relationship between microstructure and electrical properties can be obtained from complex impedance plot. The impedance spectrum is characterized by the appearance of semi-circular arcs due to different electrical microstructural contribution. The semicircle at lower frequency is due to the contribution of electrode-material interface, another semi-circular arc at intermediate frequency is due to the contribution of grain boundary, and at high frequency the semi-circular arc is due to the bulk response of the material as shown in Figure3.10. The impedance data were measures at same conditions as dielectric characterization.

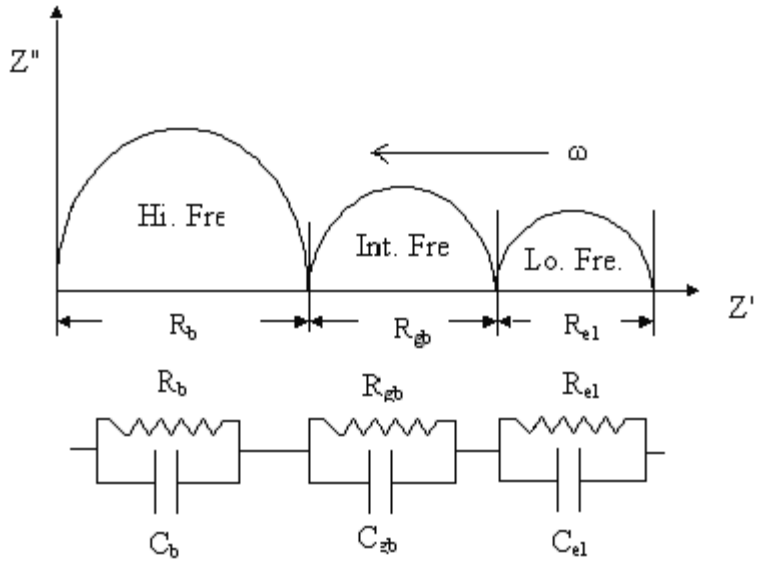

Figure 3.10: Relationship between microstructure-electrical properties in complex impedance plane and an electrical equivalent circuit in complex impedance plane. The intercept of the semi-circular arcs on the real axis gives rise to the corresponding resistances such as Bulk, GB and interfacial.

Chapter-4

Results and discussion

RESULTS AND DISCUSSION

4.1. Collection of cenosphere

Figure 4.1: Collection of cenosphere

Cenosphere has been collected from ash lagoon of TSTPS, Kanhia Odisha. Cenosphere is collected from ash dyke by gunny bags.

4.2 Particle size analysis

The particle size distribution (PSD) of a powder, or granular material, or particles dispersed in fluid, is a list of values or a mathematical function that describes the relative quantities of particles exist, sorted according to size. PSD is also known as grain size distribution.

A better indication of the fineness is to determine the particle size distribution. Particle size distribution of the cenosphere sample obtained from dry sieving and using a laser particle size analyzer. Cenosphere sample consists of particles with diameter ranging from 0.065mm to 0.160mm. However, few particles with maximum diameter of 0.350 mm and minimum diameter of 0.0005 mm are noticed in the sample. From the Figure 4.2 it has been found that the mean diameter of the cenosphere particle is 0.117mm. Cenosphere have the following distribution: 0.02-0.4% of cenosphere particles are found below .001 mm and 1.2-1.5 % particles lie in the range of 0.001mm - 0.010 mm. Higher percentages (nearly 44%) of particles lie in the range of 0.010mm to 0.100mm. Nearly 40% of particles, in the range between 0.100mm to 0.250mm give the solid evidence regarding the bulkiness of the light weight particles. The above data are shown in Figure 4.2. They are larger in size than that of fly ash particle (from Figures 4.2 and 4.3). Due to the entangled air inside the rigid sphere,

the diameter of the fly ash cenosphere is increased. The size ranges of the cenosphere particles can be specified by dispersion strengthening composite as well as particle reinforced composite. Thus the strengthening of composite can be attained due to dispersion strengthening along with particle reinforcement.

The particle size distribution of the fly ash particle is shown in Figure 4.3. The fly ash particles are much smaller as compared to cenosphere. The minimum and maximum sized fly ash particles lie in the range between 0.0015mm to 0.08mm (as compared to 0.0005 to 0.350). The mean diameter size of fly ash particle and cenosphere are 0.0075mm and 0.117mm respectively (Figures 4.2 and Figure 4.3). From these figures it is observed that cenosphere particles are much larger than that of fly ash. It is also revealed that the particle size of cenosphere is about 25% of the particle size range of fly ash.

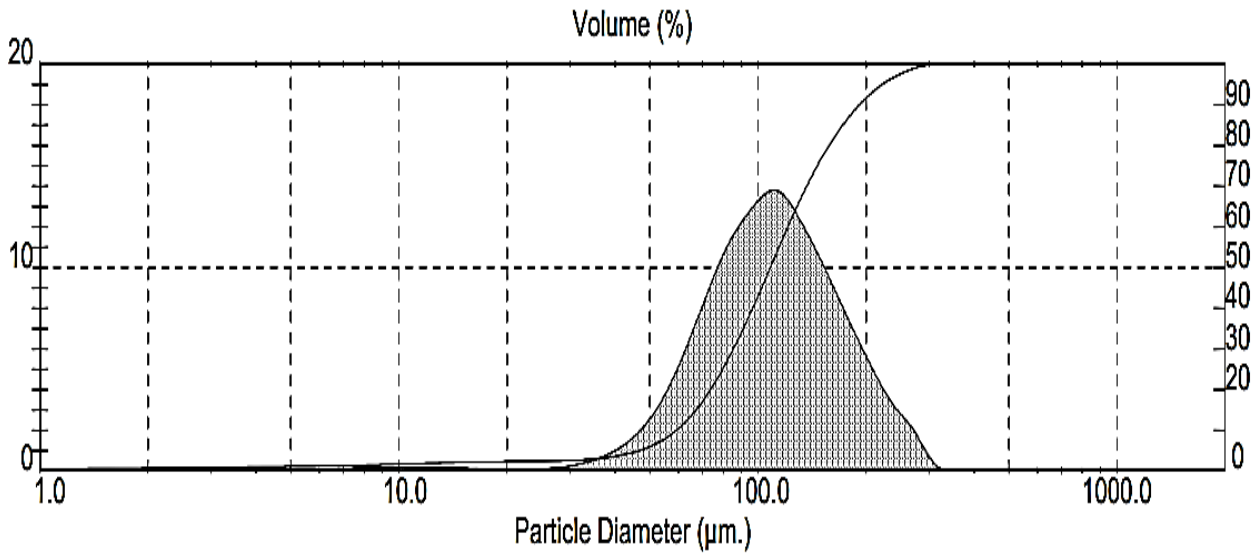

Figure 4.2 Particle size analysis of cenosphere.

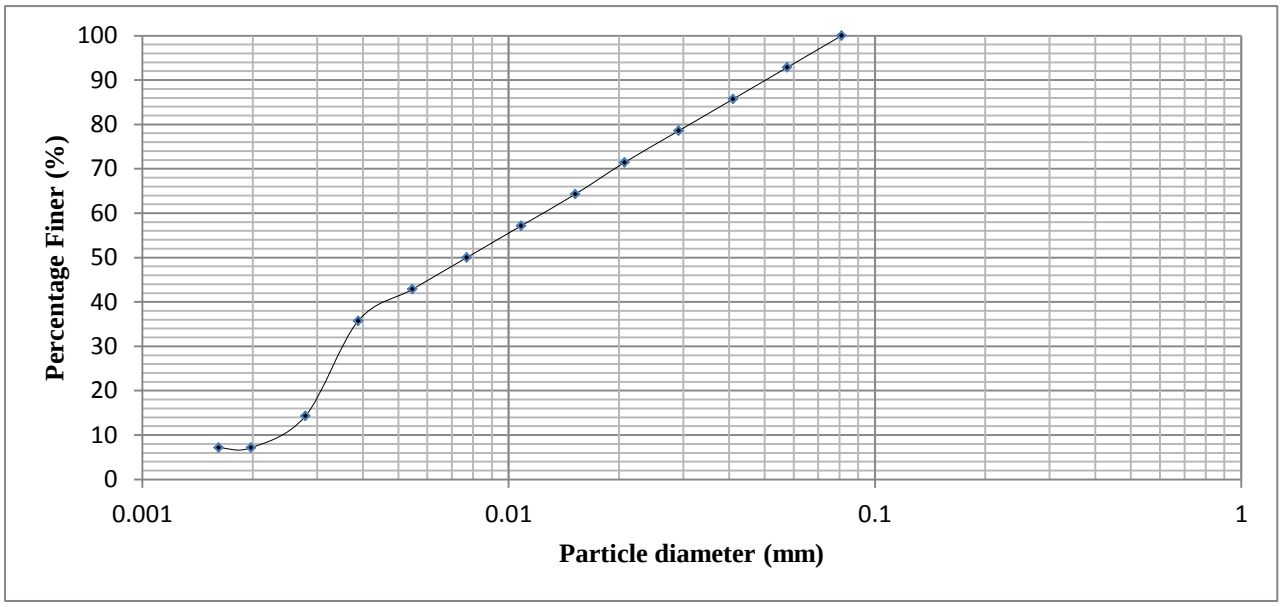

Figure 4.3: Particle size distribution of fly ash

4.3 Specific Surface Area

The specific surface area of cenosphere has been found out to be 62.45m^2/kg by using equation 3.1. The specific surface of fly ash has been found out to be 293.15m^2/kg. This confirms that the specific surface area of cenosphere is much less than fly ash. The lower specific surface area value shows the presence of regular larger spherical sizes. Fly ash particles are much finer and have lesser particle diameter than that of cenosphere. So the light weight particle like cenosphere has lesser value of specific surface area due to its larger size. A large value of interstitial void space is found in the floating particle like cenosphere. Due to this large value of interstitial spaces between the individual particles there is much higher speed of airflow that occurred inside the Blain's specific surface area measuring device which gives rise to rapid flow of light grade mineral oil. This regular individual spherical size of cenosphere has higher porous value for which it is used in acoustical panels, sound proofing materials and body fillers.

4.4 Compaction characteristics

The compressive strength of cenospheres samples are determined under INSTRON machine. The cenosphere samples are prepared under 6 tons and 4 tons pre-loadings. After preparation samples are tested under INSTRON. The results obtained in both cases are mentioned below.

Table 4.1: Compressive Strength for 6 ton cenosphere pellets

Height (mm)	Diameter (mm)	Compressive Strength (MPa)	Average Compressive Strength (MPa)
7.87	15.02	7.39	7.38
7.88	15.01	7.37	
7.89	15.02	7.37	

Table 4.2: Compressive Strength for 4 ton cenosphere pellets

Height (mm)	Diameter (mm)	Compressive Strength (MPa)	Average Compressive Strength (MPa)
7.02	15.02	6.14	6.14
7.25	15.01	6.18	
7.22	15.02	6.10	

The compressive strength of common building bricks, second class bricks and first class bricks are 3.43MPa, 6.86 MPa and 10.29 MPa. Compressive strength of cenosphere pellet produced by 6 ton loading is around 7.38MPa. It can be used as light weight brick by addition of different additives such as sodium silicate. Good heat stability and fire resistive property make cenospheres indecomposable in high temperature on account of high fusion point. That can enhance fire resistance and heat deflection temperature. Quartz, hematite and alumina possess high compressive strength. Cenosphere contains high percentage of these minerals. So cenosphere exhibits high compressive strength property. Researchers have already found that concrete exhibits accept**a**ble level of strength properties with replacement of cement with various percentages of cenosphere. Although a decreasing strength property is observed in the composite light weight concrete but the required strength can be achieved by addition of suitable amount of additive. The addition of silica fumes to the concrete also enormously increases the strength in spite of higher percentages of cenosphere.

4.5 Compositional Analysis

The following chemical compositions of cenosphere and fly ash are found out by compositional analysis. This is mentioned in Table 4.3 and 4.4 respectively.

Table 4.3: Chemical composition (wt. %) of the cenosphere sample

Compound	Percentages
SiO_2	48.62
Al_2O_3	27.79
Fe_2O_3	3.75
Na_2O	0.86
K_2O	4.23
MgO	0.46
TiO_2	2.12
P_2O_5	7.99
LOI	4.18

Table 4.4: Chemical composition (wt. %) of the fly ash sample

Compound	Percentages
SiO_2	41.24
Al_2O_3	24.17
Fe_2O_3	2.58
Na_2O	0.53
K_2O	2.15
MgO	0.76
TiO_2	2.09
SO_3	1.07
Zr_2O_3	25.38
LOI	0.13

Cenosphere has high $SiO_2$and Al_2O_3 content. The sum total percentages of SiO_2, Al_2O_3 and Fe_2O_3arenearly equal to 90 percentages of the total composition. The cenosphere

has low CaO content (about < 1 %) and high K_2O content (> 3 %) as observed in Table 4.3. Compounds like P_2O_5, Na_2O and TiO_2 are also found in the cenosphere as seen in Table 4.3. There are some differences found in the composition of cenosphere and fly ash. Zr_2O_3 compound is found enormously higher percentages in fly ash. This compound is found only in trace amount in the cenosphere. A relatively lower percentage of quartz is found in fly ash than that of cenosphere. Nearly same amount of hematite and alumina are found in the cenosphere and fly ash. P_2O_5 compound is found only in trace amount in the fly ash but it is found as a relatively higher percentage in cenosphere.

4.6 Mineralogical composition

The following mineral compositions of cenosphere and fly ash are found out by XRD analysis. These are mentioned in Figure 4.4 and Figure 4.7 respectively. The constituents of cenospheres are depicted in Figure 4.5 and Figure 4.6. Figure 4.4 depicts the room temperature X-ray diffraction spectra of Cenosphere. It is observed that the XRD spectra are a superposition of various crystallographic phases. The mineral constituents of the materials have been reported bay Kolay *et al.* They observed the presence of the following minerals (*i.e.* quartz, mullite, sillimanite, magnetite, hematite, rutile, dipotassium oxide, calcium oxide, sodium oxide, magnesium oxide). In order to confirm the signature of reflection of the above mentioned compounds we have simulated the XRD spectra of individual constituent as shown in Fig 4.5 and Fig 4.6. Fig 4.5 and fig 4.6 clearly resisters the evidence of the mentioned mineral well with in the calculation error. We have identified all the minerals shown in Fig 4.4. It is also to be noted that primary content of the cenosphere is dominated by SiO_2.Alumina is predominantly present. These XRD graphs are mentioned below from Figure 4.4 through Figure 4.7

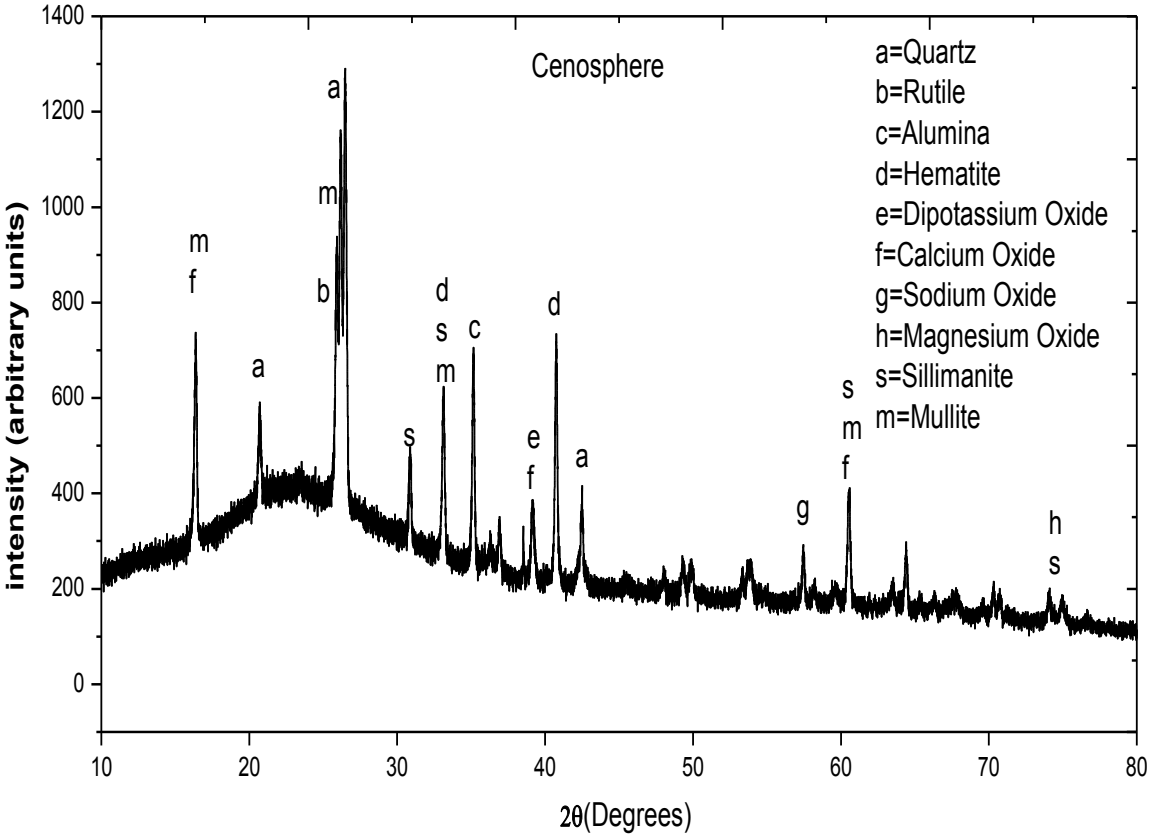

Figure4.4: XRD spectra of cenosphere

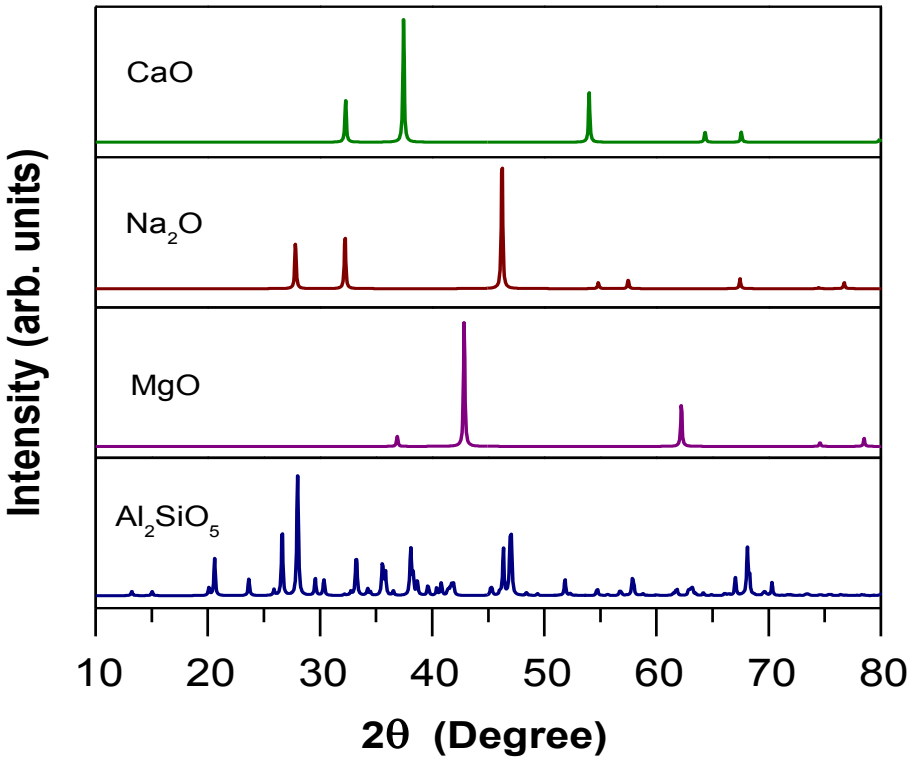

Figure 4.5: XRD diffraction spectras of constituent compounds

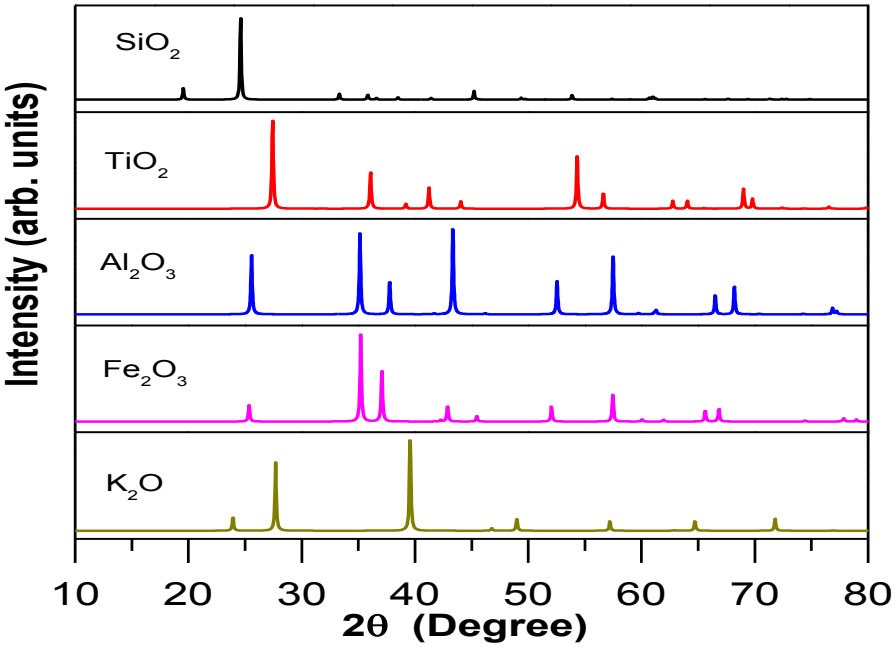

Figure 4.6: XRD diffraction spectras of constituent compounds

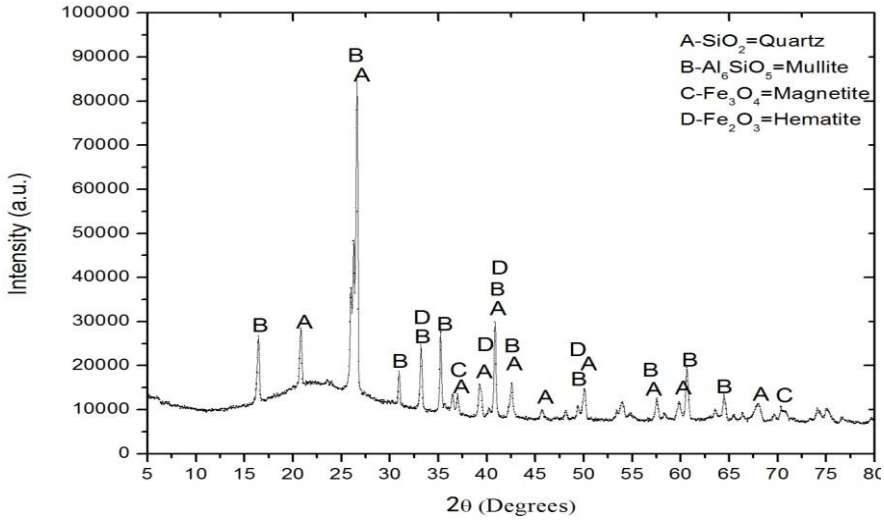

Figure 4.7: XRD diffraction spectra of fly ash

4.7 Morphological analysis

Figures 4.8 through 4.113 depict the FESEM micrographs of the cenosphere sample. From these micrographs, it can be observed that the cenosphere sample consists of almost regular spherical particles, ranging from 0.05 to 0.11mm in diameter. This is in good agreement with the particle size distribution characteristics as depicted in Figure 4.8. The average size of cenosphere particle is arround 100µm which is confirmed from figure 4.8. No cross linked structures are found inside cenosphere. From Figure 4.11 and Figure 4.13. It is found that the cenosphere shell thickness is arround 6 percent to 10 percent of the diameter. Plerosphere particle is also found in the coal ash sample brought from the site as the microsphere is filled with smaller ash particles. There are large void space found inside the cenosphere which is confirmed from Figure 4.11 and Figure 4.13. A large paercentage of interstitial void space is found in the distribution of cenosphere. Cenospheres are used in fillers for its improved flow characteristics, less shrinkage property. Some SEM and FESEM micrograph are described in Figures 4.8 through 4.13.

SEM Images:

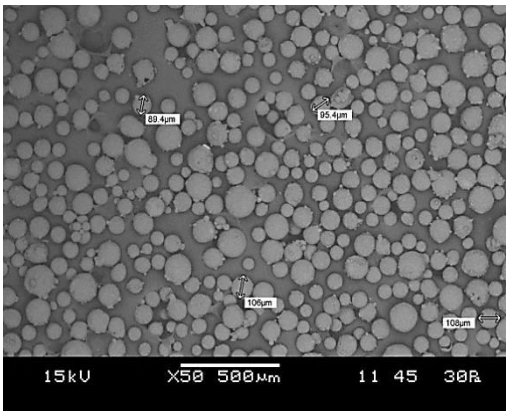

Figure 4.8: Distribution of cenosphere Matrix

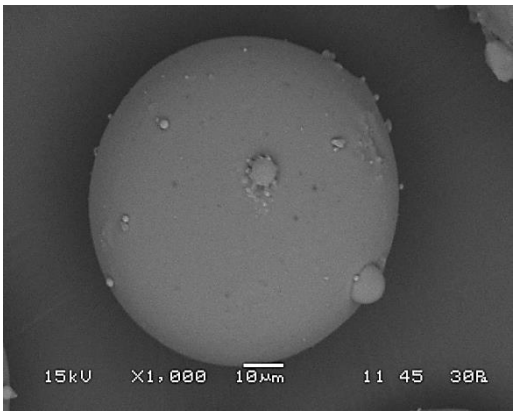

Figure 4.9: Average size of cenosphere

FESEM Images:

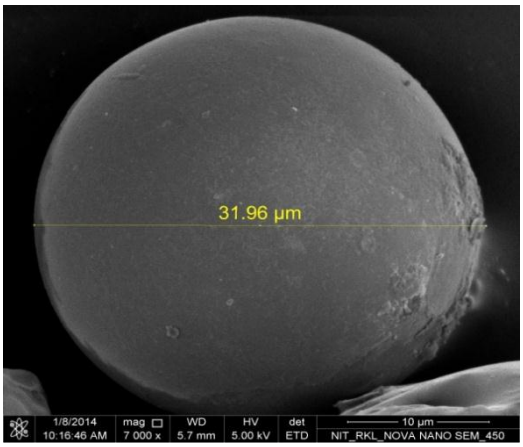

Figure 4.10: Cenosphere

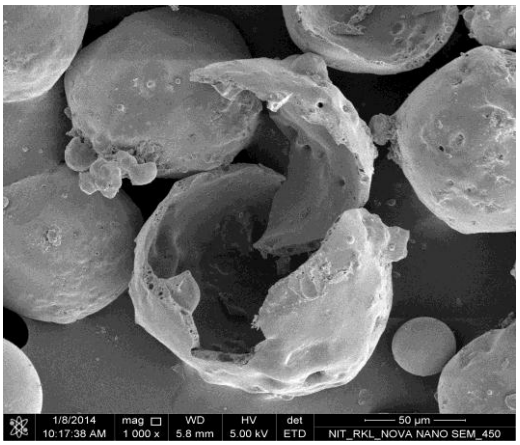

Figure 4.11: Void space of cenosphere

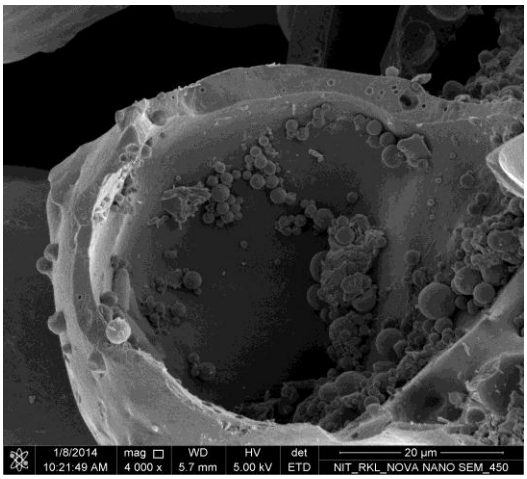

Figure 4.12: Plerosphere

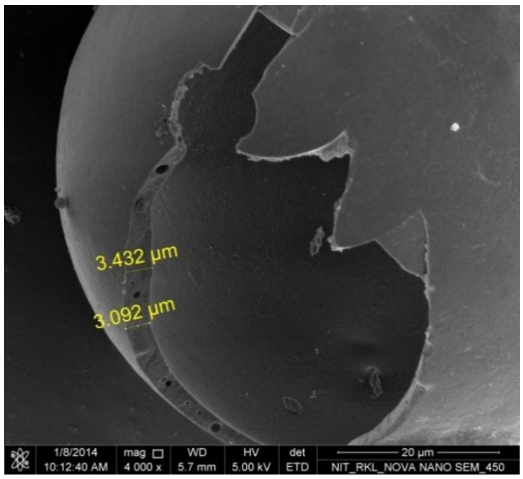

Figure 4.13: Thickness of cenosphere shell

4.8 EDS of cenosphere

Figure 4.14 and Figure 4.15 shows the energy dispersive X-ray analysis (EDS) of cenosphere. In Figure 4.14 and Figure 4.15, the intermixing of Fe and Al-Si mineral phases are shown. The fly ash and cenosphere samples contain mainly amorphous alumino-silicate spheres and a lesser percentage of iron-rich spheres. The majority of the iron-rich spheres comprised of two phases: an iron oxide mixed with amorphous alumino-silicate. The calcium-rich material was distinct in both elemental composition and texture from the amorphous alumino-silicate spheres. Oxides of Fe, Na, K, Mg minerals are present in traces in the microsphere sample. Zr oxides of fly ash shows relatively higher peak value than oxsides of cenosphere. These are EDS images of cenosphere and fly ash depicted through Figure 4.14 and Figure 4.15.

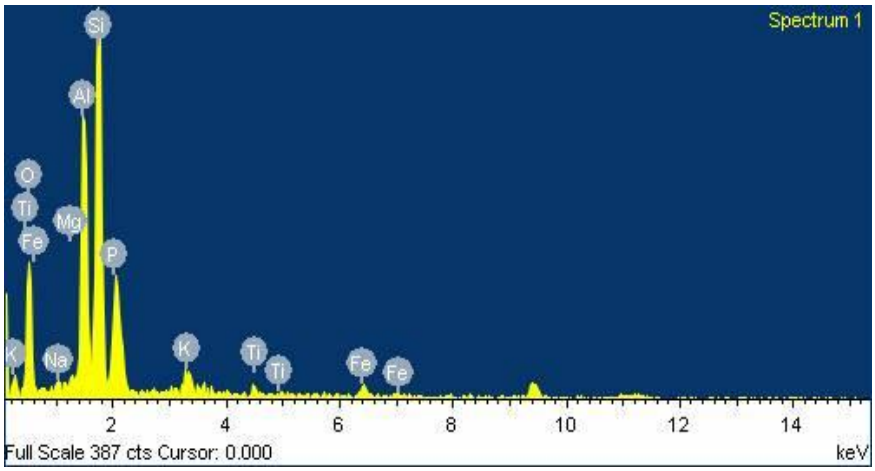

Figure 4.14: EDS of cenosphere

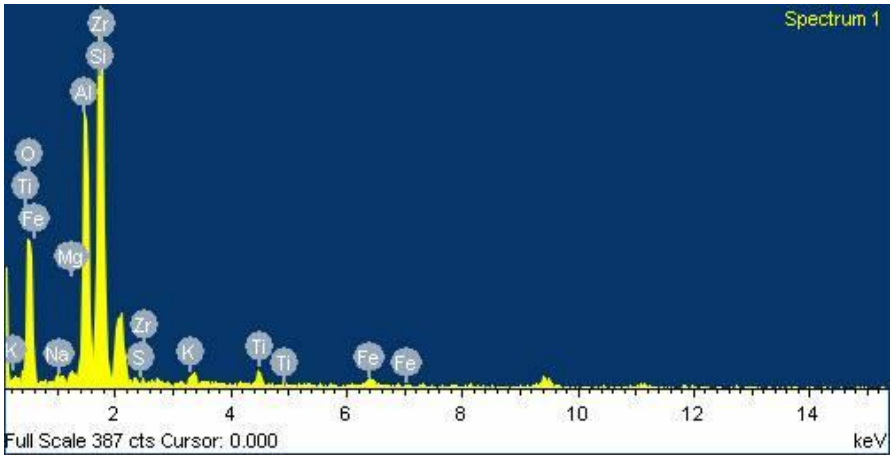

Figure 4.15: EDS of Fly ash

4.9 Thermal analysis

TGA and DTA thermogram of cenosphere is observed in Figure 4.16. Figure 4.16 shows the DTA-TGA thermogram of cenosphere at N_2 atmosphere with temperature range RT-1000^{0}C. It is observed that with increase in temperature an anamoly is observed at TGA pattern at 100^{0}C which is accompanied by an endothermic peak in DTA pattern. This corresponds to water loss. Further increase in temperature above 250^{0}C, another slope change in DTA pattern and remarkable mass losses in TGA is observed at 300^{0}C which may be due to evaporation of carbonaceous substance. Further increase in temperature to 1000^{0}C hardly any change is observed in thermal pattern. It is to be noted that 1.5% of mass is loss during the temperature range of 1000^{0}C and this signifies the higher thermal stability of the material. The figure below depicts TGA and DTA thermogram.

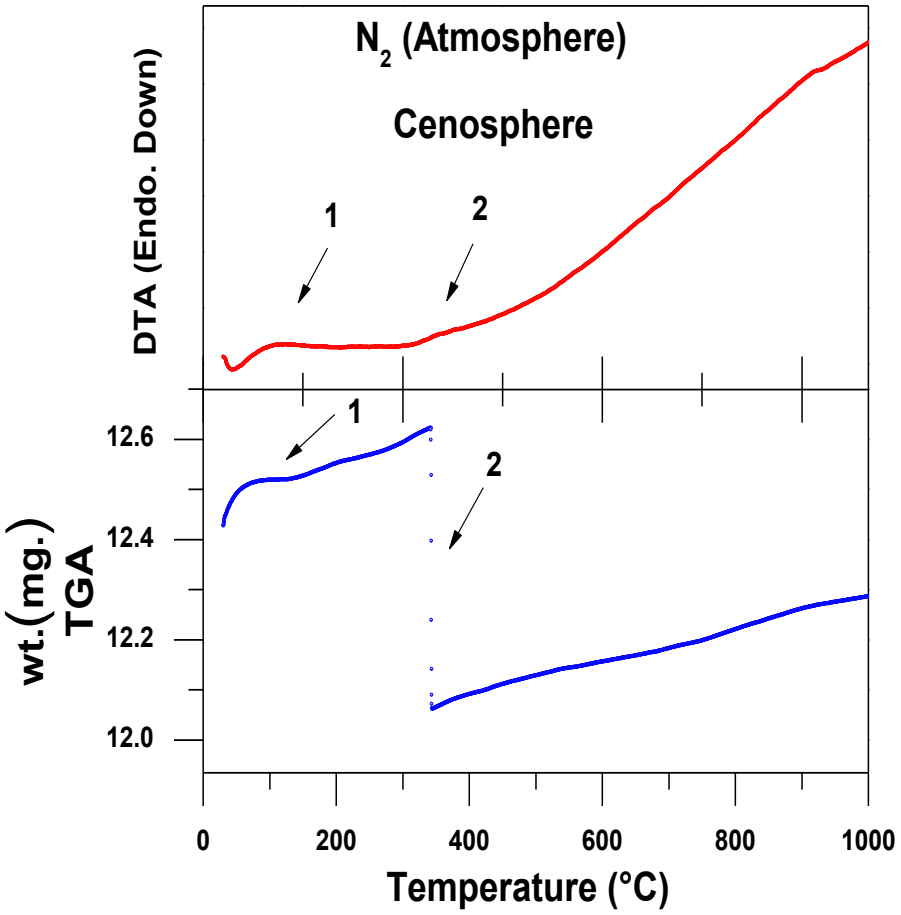

Figure 4.16: TGA and DTA pattern of cenosphere sample

4.10 Electrical Resistivity and Dielectric spectroscopy

The following Figures from 4.17 through 4.19 show the dielectric permittivity and electrical resistivity properties of cenosphere. Figure 4.17 shows the frequency dependence of dielectric permittivity and loss tangent. It is observed that dielectric permittivity decreases with increase in frequency. This is a characteristic of polar material. Similar type of behaviour is observed in loss tangent. The magnitude of loss tangent varies with the range between 0 and 0.5 indicating low dissipation factor.

In order to further investigate the bulk resistance of material, the nyquist plot (Z imaginary vs. Z real) is demonstrated in Figure 4.18. The above data is fitted with an R-C

circuit and estimated bulk resistance to be 2.26 × $10^{8}\Omega$ and the capacitance 4.48 × 10^{-11}F. This signifies higher magnitude of bulk resistance.

The Figure 4.19 shows the equivalent R-C circuit plotted between the imaginary part of impedance and phase angle as a function of frequency. It is observed that imaginary part decreases monotonically with increase in frequency. This graph shows a single relaxation curve. These are graphical representations of resistivity properties of cenosphere.

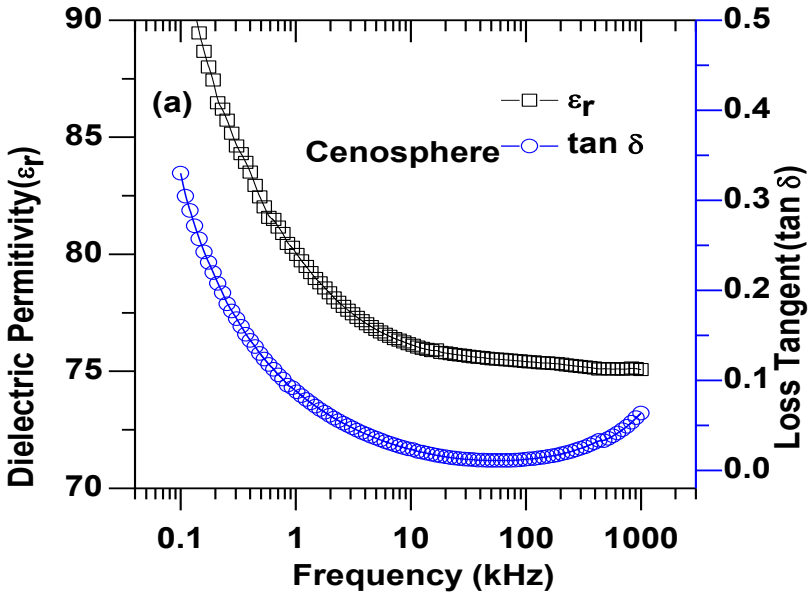

Figure 4.17: Dielectric permittivity and loss tangent of cenosphere

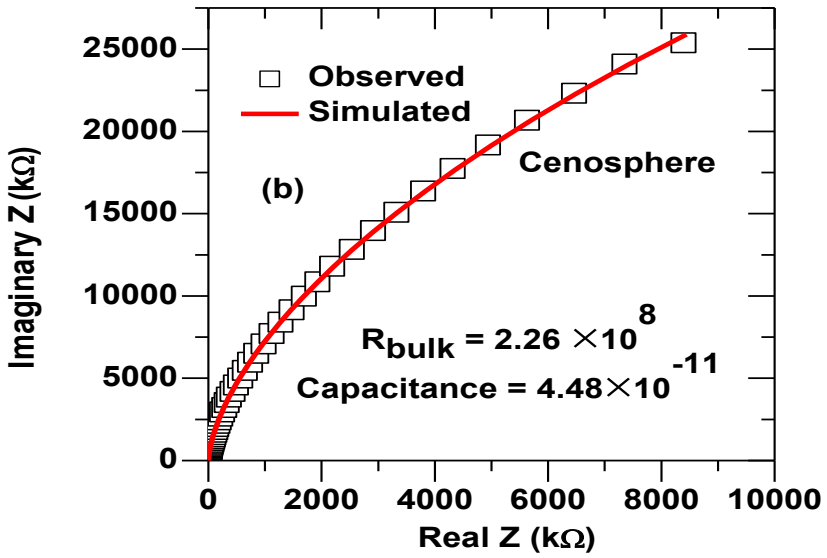

Figure 4.18: Electrical resistance and capacitance of cenosphere

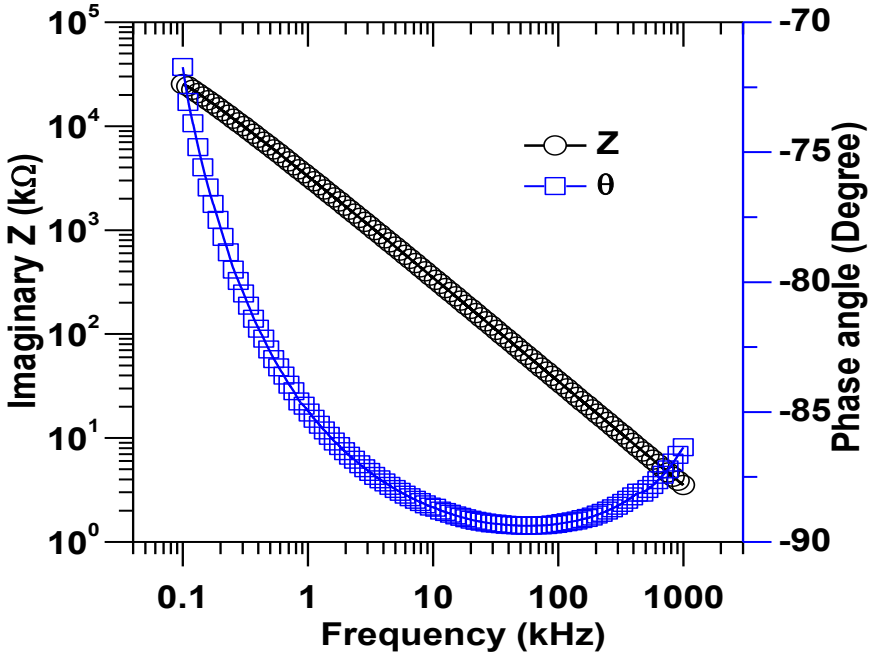

Figure 4.19: Complex impedance and phase angle of cenosphere

CONCLUSION

In the present work, cenosphere sample is collected from NTPC, Kanhia and it is processed with suitable reagent for further characterization study. The mineralogical, morphological, electrical (dielectric and impedance), thermal properties of the light weight hollow particle have been studied extensively. Apart from this the particle size distributions, compositional analysis, surface area of the compound have been studied.

Based on our results the following conclusions have been made.

1. The particles are almost all uniform in size and the specific surface area is quite less due to their larger size.
2. Cenosphere sample consists of particles with wider range between0.005mm to 0.035 mm . The mean diameter of the cenosphere particle is 0.117mm.
3. The cenosphere particle exhibits higher compressive strength (7.38MPa).
4. Quartz and alumina are most abundant minerals in cenosphere. Quartz, alumina and hematite conclude the maximum percentages (nearly 90%) of the total composition.
5. Cenosphere particles achieve very high electrical resistivity ($R=2.26*10^{8}\Omega$) property. Cenosphere can be used as insulating material.
6. Cenosphere particle is stable up to higher temperature ($1000^{0}C$) with a negligible mass loss.
7. Cenosphere comprised of hollow sphere having wall thickness around 10 percentages of the spherical diameter. There is no sign of cross linked structure in side this cenosphere. Larger interstitial spaces are found in distribution of cenosphere. Due to the higher porous nature it can be effectively used in acoustic panel.

References

1. Wang, J., Zhang, M., Li, W., Chia, k., and, Liew, R. (2012). Stability of cenospheres in lightweight cement composites in terms of alkali–silica reaction. *Cement and Concrete Research, 42*, 721–727.
2. Y, X., Shen, Z., Xu, Z., and, Wang, S. (2007).Fabrication and structural characterization of metal films coated on cenosphere particle by magnetron sputtering deposition. *Applied Surface Science, 253*, 7082-7088.
3. Cao, X., and, Zhang, H. (2013).Investigation into conductivity of silver-coated cenosphere composites prepared by a modified electroless process. *Applied Surface Science, 264,* 756-760.
4. Das, A., and, Satapathy, B.K. (2011).Structural, thermal, mechanical and dynamic mechanical properties of cenosphere filled with polypropylene composites. *Materials and Design, 32*, 1477-1484.
5. Wang, M., Jia, D., He, P., and, Zhou, Y. (2011). Microstructural and mechanical characterization of fly ash cenosphere/metakaolin based geopolymeric composites. *Ceramics International, 37,* 1661-1666.
6. Meng, X., Shen, X., and, Liu, W. (2011).Synthesis and characterization of Co/cenosphere core-shell composites.
7. *Applied Surface Science, 258,* 2627-2631.
8. Fenelov, V.B., Mel'gunov, M.S., and, Parmon, V.N. (2010).The properties of cenosphere and the mechanism of their formation during high temperature coal combustion at thermal power plants. *KONA Powder Particle Journal No. 28,*189-208
9. Vassilev, S.V., Menedez, R., Somano., and, M.D., Tarazona, M.R. (2004). Phase-mineral and chemical composition of coal fly ashes as a basis for their multicomponent utilization. 2. Characterization of ceramic cenosphere and salt concentrates. *Fuel, 83,*585–603.
10. Meng, X., Li, D., Shen, X., and, Lu, W. (2010).Preparation and magnetic properties of nano-Ni coated cenosphere composites. *Applied Surface Science, 256*, 3753-3756.
11. Zhi-qui, H., Si-rong, Y., and, Mu-qin, L. (2010).Microstructures and compressive properties of AZ91D/fly ash cenospheres composites. *Transactions of Nonferrous Metals Society of China, 20*, 458-462.
12. Dou, Z.Y., Jiang, L.T., Wu, G.U., Xiu, Z.Y., and, Chen, G.Q. (2007).High strain rate compression of cenosphere-pure aluminum syntactic foams. *ScriptaMaterialia, 57*, 945-948.

13. Ngu, L., Wu, H., and, Zhang, D. (2007) .Characterization of Ash Cenospheres in Fly Ash from Australian Power Stations. *Energy and Fuels, 21,* 3437-3445.
14. Kolay, P. K., and, Singh, D.N. (2001).Physical, chemical, mineralogical, and thermal properties of cenosphere collected from an ash lagoon. *Cement and Concrete Research, 31,*539-542.
15. Goodhew, P. J., Humpphreys, J., and,Beanland, R. (2001). Electron Microscopy and Analysis, *Taylor and Francis*.
16. Cullity, B. D. (1956). X-ray Diffraction. *Addison-Wesley Publishing Company*.
17. Speyer, R. F. (1994). Thermal Analysis of Materials, *Marcel Dekker, Inc.*
18. Kao, K. C. (2004). Dielectric Phenomena of Solids, *Elsevier Academic Press*.
19. Gerhardt R. (1994). *J. Phys. Chem. Solids, 55*, 1491.
20. Sinclair,D. C., and,West,A. R. (1989). *J. Appl. Phys., 66,* 3850.
21. Gurupira, T., Jones, C., and, Stencel, J.Cenosphere Separation from Fly Ash Using Pneumatic Transport, Triboelectric Processing.
22. Tiwari, V., Shukla, A. and, Bose, A. (2004). Acoustic properties of cenosphere reinforced cement and asphalt concrete. *Applied Acoustics, 65,* 263–275.
23. Alcala, J.F.C., Davila, R.M., and, Quintero, R.L. (1987). Recovery of Cenospheres and Magnetite from Coal Burning Power Plant Fly Ash. *Transactions ISIJ, 27,* 531-538.
24. Brown, M.E. (2001). Introduction to thermal analysis. *Kluwer*.